NOAA Technical Memorandum NWS SR-185

TECHNIQUES FOR ISSUING SEVERE THUNDERSTORM AND TORNADO WARNINGS WITH THE WSR-88D DOPPLER RADAR

Kenneth W. Falk
NWSO Shreveport, Louisiana

Scientific Services Division
Southern Region
Fort Worth, Texas

April 1997

UNITED STATES
EPARTMENT OF COMMERCE
lliam M. Daley, Secretary

National Oceanic and Atmospheric Administration
James Baker
Under Secretary and Administrator

National Weather Service
Elbert W. Friday
Assistant Administrator

TECHNIQUES FOR ISSUING SEVERE THUNDERSTORM AND TORNADO WARNINGS WITH THE WSR-88D DOPPLER RADAR

ABSTRACT

This paper reviews conventional radar warning guidelines and compiles techniques for the decision making process in issuing Doppler radar based severe thunderstorm and tornado warnings. The ideas presented in this paper are not meant to be the definitive study on the subject of radar techniques for warnings, but are only meant to be guidelines on the subject. Local warning techniques, such as vertically integrated liquid (VIL) techniques are only briefly mentioned, but the most widely used and accepted warning techniques are included in detail. The latest research on techniques for warning for non-supercell tornadoes and ordinary cell microbursts is also presented.

1. Introduction

A **severe thunderstorm** is defined by the National Weather Service as a thunderstorm that produces a tornado, and/or winds of at least 50 kt (58 mph), and/or hail at least ¾ in in diameter. Structural damage may imply the occurrence of a severe thunderstorm. A **tornado** is defined as a violently rotating column of air, pendant to a cumulonimbus, with circulation reaching the ground.

The purpose of this paper is to serve as a guideline for issuing severe thunderstorm and tornado warnings using information from the WSR-88D (**W**eather **S**urveillance **R**adar 19**88** **D**oppler) Doppler radar. I have attempted to summarize most of the published and/or accepted techniques for issuing warnings based on Doppler radar. The paper is intended to be used as an easy reference by meteorologists tasked with issuing severe weather warnings. Another possible use of this paper is for training meteorologist interns on radar warning techniques. I cannot include all local office techniques that are available, such as local vertically integrated liquid (VIL) studies, but I hope I have included the most widely used and accepted techniques.

Section 2 discusses conceptual models of thunderstorms that will be referred to throughout this paper. Section 2 blends with Section 3, which relates environmental factors to thunderstorm types and expected severe weather. Even with Doppler radar, environmental factors should be taken into account before a decision is made on the type of warning issued.

With the development of Doppler radar, new techniques have been developed in addition to the criteria that were used for conventional (non-Doppler) radars. The Doppler radar criteria do not take the place of the Lemon criteria (Lemon 1980), but add many more features that can be used to issue severe thunderstorm and tornado warnings. The Lemon criteria and the additional Doppler radar techniques are discussed in Sections 4 and 5 of this paper respectively.

recent research has produced a few techniques for warning for non-supercell tornadoes and for ordinary cell microbursts. These techniques are also incorporated into Section 5.

A summary of techniques is provided (just before the figures in the middle of the document) for quick reference.

2. Conceptual Models of Thunderstorms

Thunderstorms can be categorized according to certain characteristics they exhibit by various conceptual model, radar, or visual features. For the purposes of this paper the classifications of thunderstorms will follow the descriptions listed in this section. When the radar features or signatures of severe thunderstorms and tornadoes are discussed in later sections, references will be made to the conceptual models discussed in this section. Although these thunderstorm types are presented as distinctly different, in reality these features will usually blend into each other, or evolve from one type to another.

a. Ordinary thunderstorm

The first thunderstorm type is the ordinary (single cell) thunderstorm. This thunderstorm is characterized by the formation of a single thunderstorm updraft (as seen in Fig. 1), which is followed by a downdraft and dissipation of the thunderstorm within 1 hr (Doswell 1985). The ordinary thunderstorm can produce severe weather such as high winds or hail, but tornadoes are rare (although non-supercell tornadoes can occur). This thunderstorm type will be discussed later in the context of a severe thunderstorm, when the ordinary thunderstorm microburst radar signatures are presented (see Section 5.a.3). Forecasters can anticipate an ordinary thunderstorm microburst in a favorable environment (see Section 3.a).

b. Multicell thunderstorm

The multicell thunderstorm conceptual model is shown in Fig. 2. This thunderstorm type is characterized by multiple updrafts forming new cells as each downdraft (and precipitation) dissipates the previous cell (Ray 1986 [see Weisman and Klemp, Chapt. 15]). Cold air outflow from each dissipating cell triggers new cells along the leading edge of the outflow, generally in the direction of the storm motion. This thunderstorm type is more long-lived than an ordinary thunderstorm. The multicell thunderstorm is characterized by a strong radar reflectivity gradient on the leading edge of the thunderstorm, and possibly by a radar weak echo region (WER) just above the low level reflectivity gradient area. Squall lines usually contain several multicell thunderstorms, but can also contain embedded supercell storms (see below).

Multicell thunderstorms produce a variety of severe weather including large hail and damaging wind. Short lived tornadoes have been known to occur on the leading edge of the outflow. Generally the tornadoes that occur with multicell (or ordinary cell) thunderstorms are not as severe as the tornadoes that occur with the supercell thunderstorm.

c. Supercell thunderstorm

The supercell is generally defined as a thunderstorm with a persistent rotating updraft (mesocyclone). The supercell thunderstorm is a long-lived (over several hours time) thunderstorm with distinctive radar and visual features (Ray 1986 [see Weisman and Klemp, Chapt. 15]). The conceptual model of a supercell thunderstorm is presented in Figs. 3 and 4. In Fig. 3, the radar signatures and wind fields of a supercell thunderstorm are shown. The familiar radar reflectivity signature commonly referred to as the "hook echo" is shown to be at the confluence of the thunderstorm updraft with the rear flank downdraft, and is the preferred region for strong tornado occurrence. The hook echo is also the region where the mesocyclone will be located at the surface, or aloft, in a supercell thunderstorm.

Figure 4c shows a mature supercell and depicts supercell thunderstorm radar features such as the bounded weak echo region (BWER), the hook echo, the strong leading edge reflectivity gradient, and the thunderstorm top overhanging the low level reflectivity gradient area. The BWER and the overhanging thunderstorm top are caused by the strong, nearly vertical, updraft of a supercell thunderstorm suspending precipitation particles aloft. The hook echo and mesocyclone are caused by the tilting of horizontal environmental vorticity into the vertical causing rotation of the updraft. This is also a factor in formation of a BWER.

The supercell thunderstorm typically moves to the right of the environmental storm motion vector, thus it will appear on the radar as moving to the right of other thunderstorms that may be present. Although anticyclonic supercells can occur (moving left of the storm motion vector), they have not been associated with tornadoes as the cyclonic right moving supercell thunderstorm. Supercell thunderstorms are capable of producing strong destructive tornadoes, large hail, and damaging wind.

Three sub-categories of the classic supercell have been identified. These are the low-precipitation (LP) supercell (Bluestein and Parks 1983), the high-precipitation (HP) supercell (Moller et al. 1990), and the mini supercell (Burgess et al. 1995). The LP supercell thunderstorm (Fig. 5) is found in the surface dryline environment just east of the Rocky Mountains over the western Great Plains (Moller et al. 1994). LP supercell environments are characterized low to moderate moisture values. Severe weather with LP supercells is limited to large hail and an occasional weak to moderate tornado.

The HP supercell (Fig. 6) occurs over the central and eastern United States and may be the dominant form of supercell nationwide. This type of thunderstorm has substantial precipitation in the mesocyclone (Moller et al. 1994). The HP supercell can produce tornadoes and/or high winds. Large hail is also possible with this type of supercell, but may not be as common as with the classic or LP types of supercells.

In addition, mini supercells as described by Burgess et al. (1995) can produce severe weather. Mini supercells are smaller than traditional supercells in both horizontal and vertical extent but still possess the same radar attributes, including hook echo, well defined weak echo region, bounded weak echo region, and mesocyclone. These are also referred to as low topped supercells because the tops of these storms are lower than 30,000 ft.

d. Bow echo thunderstorm

Another type of thunderstorm is the "bow echo" thunderstorm. The name "bow echo" is derived from a rather steady state radar signature in the shape of a bow as seen in Fig. 7 (Fujita 1978). The persistence of the echo is caused by new updrafts forming on the leading edge of the bow echo. The bow echo is also characterized by bookend vortices. One bookend vortex occurs on the north side of the bow echo and contains cyclonic vorticity, while the other bookend vortex is located on the south side of the bow echo and has anticyclonic vorticity. Isolated tornadoes can occur in the cyclonic vortex of the bow echo.

The high winds that can occur with the bow echo usually are located in the rear of the center of the bow and are caused by horizontal buoyancy gradients along the rear edge of the buoyant plume aloft and cold pool near the surface generating horizontal vorticity, and accelerating the flow from rear to front at middle levels (Fig. 8, Weisman 1993).

The bow echo thunderstorm has been described as a type of HP supercell (Moller et al. 1990); however, in this paper I prefer to categorize the bow echo thunderstorm as an entity of its own.

e. Non-supercell tornadoes

A special case of severe event is the non-supercell tornado. These tornadoes occur in nonmeso-cyclone convection in an environment of weak shear over a boundary that is a source of vertical vorticity (Brady and Szoke 1989; Wakimoto and Wilson 1989). The tornado occurs in the development phase of the thunderstorm with the updraft of the thunderstorm stretching the environmental vertical vorticity.

A conceptual model of the non-supercell tornado is shown in Fig. 9. The figure depicts the source of vertical vorticity being stretched in the vertical by the convective updraft. The tornadoes caused by this mechanism are thought to be mostly F0 and F1 in intensity, but Wakimoto and Wilson (1989) have suggested that F3 damage is possible. The non-supercell tornado is generally short lived, only 5 to 10 min, but a few may last as long as 20 min.

3. Environmental factors versus storm type and severe weather

This section provides a brief discussion of some of the more commonly used environmental parameters and how they relate to storm type and severe weather. The first part discusses the ordinary cell microburst environment. Next is a section on tornado forecasting parameters, followed by a discussion on middle level winds and expected severe weather. A checklist of parameters correlated with derecho (and bow echo) formation is then presented. Lastly, results of numerical modeling of environment versus storm type are discussed.

Several environmental parameters have been correlated with severe thunderstorm and tornado occurrence. One such parameter is **convectively available potential energy (CAPE)**, defined as the positive area on a sounding associated with the buoyant part of a lifted parcel ascent between the level of free convection and the equilibrium level.

Many meteorologists refer to a parameter called storm-relative environmental **helicity** (hereafter referred to as helicity). Helicity is usually determined in the lowest 3 km of the atmosphere and is defined as:

$$\text{Helicity} = \int \mathbf{w} \cdot (\mathbf{V} - \mathbf{V}_s)dz \tag{1}$$

where $\mathbf{w} = \mathbf{k} \times d\mathbf{V}/dz$, $\mathbf{V}$ is the wind velocity, and $\mathbf{V}_s$ is the storm velocity (Colquhoun and Riley 1996). This parameter attempts to measure the amount of shear a thunderstorm experiences relative to storm motion.

Weisman (1996) presents an interesting discussion on the **role of wind shear versus helicity** in severe storms. He discusses the premise that the steadiness and propagation (right mover or left mover relative to mean flow) of supercells are a direct result of the development of rotation in the storm.

The **steadiness and propagation of supercells** are caused by an updraft that generates vertical vorticity in the middle levels of the storm due to tilting of environmental horizontal vorticity in a vertically sheared atmosphere. The vertical vorticity produces vertical pressure gradients within the storm that force the updraft to move toward a particular flank, which leads to a continuing updraft regeneration and propagation.

Helicity can only be applied to a particular storm motion, and thus storm motion must have already been observed or anticipated before helicity can be determined. In other words, helicity cannot be used directly to predict potential storm structure or motion from a given environment. **Weisman contends that supercell propagation and dynamics are similar for both straight and curved hodographs. The important factors in predicting supercells are low level wind shear and depth of shear.**

To quote from part of Weisman's article (emphasis added):

> I believe that the **vertical wind shear** perspective is superior (to helicity), because it establishes the kind of physical cause and effect link between storm structure and the pre-storm environment that forecasters can readily apply when attempting to assess storm potential on any given day. To the degree that the pre-storm environment is known and that convection is going to occur, a forecaster can simply look at the hodograph and determine to a good approximation whether there is **sufficient shear over a sufficient depth to promote supercell development (e.g. 20 ms^{-1} of wind variation over the lowest 4-6 km AGL),** whether there will be symmetric splitting or preferred flank development, and even roughly what the range of storm motions will be for the ordinary cell versus supercells. As is depicted in

> even simple simulations, supercell genesis should be viewed as a process that includes not only the development of a single, right moving, cyclonically rotating updraft, but may also include an anticyclonic left-member in some cases, or multiple cell regeneration along the surface outflow in other cases. Only from this perspective can a forecaster properly interpret the complex evolutions apparent on the radar scope. (Weisman 1996)

Other parameters will be discussed below in the tornado environment section.

a. Ordinary cell microburst environment

A special environmental case is the atmospheric condition associated with the ordinary cell microburst. This type of microburst can be sub-categorized into dry-microbursts (Wakimoto 1985) and wet-microbursts (Atkins and Wakimoto 1991).

Dry-microbursts are usually seen over the High Plains and are defined as microbursts that have little or no rain during the period of high winds. The atmospheric conditions that support dry-microbursts can be best described by model soundings as seen in Fig. 10a (Atkins and Wakimoto 1991). This type of environment is characterized by very dry air in the sub-cloud layer.

A thunderstorm that develops in this environment can enhance its severity when downdraft strength is increased by the evaporative cooling that occurs as the rainy downdraft falls through the dry air just above the surface. Convective cells in this environment can produce damaging microbursts even though updraft strength may be weak. Generally this environment is characterized by lower values of CAPE and weak vertical wind shear (Ray 1986 [see chapter 15, Weisman and Klemp]).

Wet-microbursts are more common in the more humid regions, especially the southeast U.S. Wet-microburst atmospheric and radar characteristics differ from dry-microbursts by having shallow sub-cloud layers, higher radar reflectivities, and an environmental sounding that is more statically stable. The model soundings for wet-microbursts are shown in Fig. 10b (Atkins and Wakimoto 1991). One of the interesting environmental factors discussed in Atkins and Wakimoto (1991) is that on days favorable for wet-microbursts, the change in equivalent potential temperature ($\Delta\theta_e$ = the difference between the maximum θ_e found just above the surface and the minimum θ_e aloft) must be at least 20 deg C (Fig. 10b).

b. Tornado forecasting

Recently, research has focused on a few parameters which seem to correlate better with the formation of supercells. One such parameter is the **bulk Richardson number, BRN**, which is defined to be:

$$BRN = \frac{B}{1/2 \ U_s^2} \qquad (2)$$

where B is buoyant energy in the storm's environment (CAPE), and U_s is the shear represented by the straight vector difference between the 0 - 6 km AGL mean wind and the boundary layer wind (m/s) (Weisman and Klemp 1984). BRN is readily available operationally from the SHARP program (Hart and Korotky 1991). Since supercells have been correlated with the formation of tornadoes, there is some relationship between BRN and tornado occurrence; however, tornadoes occur with non-supercells as well.

Vertical wind shear structure is also a key factor is determining tornadic potential. Several different methods of correlating vertical wind shear to supercells (and/or tornadoes) are presented here. Davies and Johns (1993) showed that both (1) the wind profile in the low levels (storm inflow layer), and (2) the strength of the wind field and shear extending through a deeper layer of the troposphere are important to supercell tornado development. Average positive (veering with height) mean shear magnitudes ($\times 10^{-3}\ s^{-1}$) were computed for 242 tornado cases:

0 - 2 km average positive shear	13.6
0 - 3 km average positive shear	10.7
0 - 4 km average positive shear	9.1

Figure 11 shows the distribution of U_s (0 - 6 km shear) for the Davies and Johns dataset. The majority of the cases (70 percent) were associated with U_s values greater than 18 ms^{-1}. Figure 12 shows the distribution of BRN for the same dataset (Johns et al. 1993). From the graph it is easy to see that BRN values under 20 were a significant supercell (possibly tornadic) threat. And in Fig. 13, tornado cases are plotted on a CAPE versus shear diagram. Most cases had CAPE under 3,200 and 0 - 2 km shear higher than $9 \times 10^{-3}\ s^{-1}$. As previously discussed, Weisman (1996) states that in the lower 4 - 6 km of the atmosphere, vertical wind shear of 20 ms^{-1} or more is sufficient for supercell development (and possibly tornadoes).

c. *Middle level winds and expected severe weather*

An interesting discussion of the different vertical wind profiles between tornadic and nontornadic supercell environments is provided by Brooks et al. (1994). The authors show that low level tornadic mesocyclones develop by different processes than middle level mesocyclones. They propose that CAPE and low level shear (or helicity) do not adequately describe the differences between tornadic and nontornadic supercell environments, but that differences in middle level storm relative winds may provide a clue to the environment that may produce tornadic supercells. In their discussion, middle level winds are defined as those between 6,000 and 28,000.

The authors suggest for very weak middle level storm relative environmental winds, any low level mesocyclones will occur early in the storm's life and be short lived, with the outflow dominating the storm (especially in a high CAPE environment). For very strong middle level storm relative winds, the low level mesocyclone would be very slow to develop or perhaps not develop at all. For moderate middle level storm relative winds, long-lived low level mesocyclones might result if the mesocyclone circulation and storm relative middle level winds are balanced in some sense. The results of their research is shown in Fig. 14, where q(max) is the maximum water vapor content in the boundary layer (g/kg), and H / v(min) is the ratio of 0-3 km helicity to the minimum storm relative wind (m/s) averaged over a depth of 1 km in the 6,000 to 28,000 ft layer. The reader is referred to the article for further information.

d. Derecho checklist

Derechos have become more recognizable as another form of severe weather. Derechos are defined to be widespread, rapidly moving, convectively induced windstorms that produce significant damage and often casualties. Johns and Hirt (1987) provided a list of environmental factors favorable for the formation of derecho type damaging windstorms. The guidelines from Johns and Hirt have been put in a checklist format (Fig. 15) for easy reference. One type of thunderstorm that occurs often in derechos is the bow echo type storm, so this checklist will also aid the forecaster in determining if the environment is favorable for bow echoes.

e. Numerical modeling of environment versus storm type

While the thermodynamics of the environment are important in determining updraft strength, vertical wind shear has a strong influence on thunderstorm structure. Figure 16 correlates the relationship between wind shear and storm type. These composite hodographs are for environments typical of ordinary cells, multicell storms, and supercell storms.

In the case of little vertical wind (Fig. 16a), a thunderstorm will produce an outflow that will move across the surface equally in all directions. But with little wind to move the thunderstorm, the outflow will cut off the inflow of moist and unstable air, and further updraft development is stopped (Ray 1986 [see Chapter 15, Weisman and Klemp]).

In the case of increased shear of Fig. 16b, both multicell and supercell storms can occur. An explanation for this is presented by Rotunno et al. (1988). Figure 17 shows the theory that the essential factor of a long lived multicell thunderstorm (or line of thunderstorms) is the amount of low level shear that counteracts the circulation induced by the thunderstorm outflow. The outflow is produced by precipitation evaporating as it nears the surface. With shear and outflow (Fig. 17d), there is a balance of the circulation generated by the outflow with the environmental circulation generated by environmental shear. These circulations complement each other to enhance development of new thunderstorm cells. Rotunno et al. (1988) further state that this can cause either long-lived squall lines of multicell storms, or lines of nearly steady supercells (with the supercells separate from each other along the line). The squall line occurs when the low level environmental shear is directed perpendicular to the line, with weak shear aloft. The line of supercells occurs when strong deep environmental shear is directed at an angle to the line, which allows each cell to persist without interference from other supercell storms.

In the cases of stronger vertical wind shear (Figs. 16b and 16c) horizontal vorticity inherent in the environmental flow will be tilted into the vertical by the updraft causing rotation of the updraft. The rotation produces a pressure deficit through the middle levels of the storm (4-6 km) if the vertical wind shear is deep enough. This low pressure area enhances the vertical updraft. Supercells are formed by these dynamic pressure differences (Ray 1986 [see Chapter 15, Weisman and Klemp]). The straight line hodograph in Fig. 16b favors splitting (cyclonic and anticyclonic) supercells or multicell storms, while the curved hodograph in Fig. 16c favors a dominant right-moving cyclonic supercell.

Numerical modeling of the dependence of updraft development and motion in varying vertical wind shears (hodographs) has been done by Weisman and Klemp (Ray 1986, see Chapter 15). Results were obtained from a typical severe weather type sounding shown in Fig. 18, which had a CAPE of about 2200 m^2s^{-2}. The study modeled thunderstorm structures which result from varying hodograph shapes and magnitudes. In Figs. 19A-F, "R" is the bulk Richardson number (BRN) described above. As the hodograph varied, the model produced:

Case A: Short lived multicell
Case B: Supercell on the south end of a multicell line
Case C: Curved hodograph - Right flank supercell split from weaker left flank storm
Straight hodograph - Right and left flank supercells
Case D: Right flank supercell
Case E: Weak squall line
Case F: Squall line: spearhead echo evolving into bow echo and comma echoes

The warning meteorologist can use this study as a first guess as to what type of storm to expect in a particular environment. Further study on numerical modeling of storms is available through the **Forecasters Multimedia Library—A Convective Storm Matrix: Buoyancy/Shear Dependencies**, which is a CD-ROM computer based training program (UCAR/COMET 1996).

4. Warning Criteria for Conventional Radar

Les Lemon (1980) provided a study of warning identification techniques and warning criteria for conventional radar. These techniques were generally accepted as the warning criteria used by the National Weather Service (Fig. 20). Some meteorologists may have assumed with the installation of the WSR-88D Doppler radar the Lemon criteria for warnings using conventional radar were obsolete. This is not so! The Lemon criteria are still valid warning criteria and can be used with the additional warning guidelines for Doppler radar (Section 5). In fact, some of the WSR-88D algorithms were designed to incorporate features of the Lemon criteria.

The Lemon criteria (reflectivity) can be used as confirmation of WSR-88D Doppler velocity signatures, but occasionally (without confirmation from Doppler velocity products) will be the only indication of a severe thunderstorm. The first four criteria are indicative of updraft strength. The height of the 50 dBZ echo generally applies to warning for hail, but the 27,000 ft AGL height is flexible. During the warmer months this height can be 35,000 ft AGL or higher (especially in more tropical environments) before the updraft is considered strong enough for ¾-in hail formation. This is likely due to the high freezing level during summer. Criteria 2, 3, and 4 also apply to updraft strength. Middle level echo overhang in a thunderstorm is an indication that the updraft is strong enough to suspend precipitation particles aloft (Fig. 4b).

The two Lemon criteria required for a tornado warning are both indicative of a rotating updraft (Fig. 4c). The low level pendent (hook echo) is an indication that precipitation particles are wrapping around the rotating updraft. A bounded weak echo region (BWER) detected by radar indicates a strong updraft with precipitation particles wrapped around it in the lower to middle levels of the storm (mesocyclone). These features can be verified (or enhanced) by using WSR-88D Doppler velocity products.

Meteorologists should consider Lemon criteria as guidelines for severe thunderstorm and tornado warnings as well as the more modern Doppler radar reflectivity and velocity techniques shown in Section 5. The Lemon criteria will be incorporated in Section 5 as warning guidelines for severe thunderstorm and tornado warnings.

5. Techniques for severe thunderstorm and tornado warnings using the WSR-88D Doppler radar

The techniques for severe thunderstorm and tornado warnings will be presented separately, with severe thunderstorms discussed first and tornadoes second. For severe thunderstorm warnings (under the section of hail only), a short discussion of vertically integrated liquid (VIL) will be included.

Severe thunderstorm warning techniques will be split into guidelines for hail, strong straight line wind, and ordinary cell microbursts. Tornado warning techniques will be separated into supercell and non-supercell.

These techniques are not meant to be the definitive study on the subject of severe thunderstorm and tornado warnings, but are presented as a compilation of guidelines that have been published or presented prior to the publication of this paper.

a. Severe thunderstorm warnings

(1) Hail

The techniques for **hail** are:

(1) Lemon criteria - Fig. 20
(2) Flare echo - Color Plate A1
(3) WSR-88D Doppler radar hail algorithm products
(4) Storm top divergence - Fig. 21
(5) Moderate to strong mesocyclones with environmental factors that limit tornado development - Fig. 22
(6) VIL of the Day - Fig. 24
(7) VIL of the Day equation (Eq. 3)
(8) VIL density (Eq. 4)

The Lemon criteria (Fig. 20) can be used with Doppler radar for predicting **hail**. Of particular interest is the height of the 50 dBZ echo. Lemon criteria call for a 50 dBZ echo height of at least 27,000 ft AGL for large hail (at least ¾-in diameter). This criteria can be adjusted on a daily basis similar to the way the "VIL of the Day" would be. The criteria listed in Lemon's items 2, 3, and 4 of Fig. 20 can still be used when examining Doppler radar data. These guidelines give the radar operator an indication of updraft strength in a thunderstorm. The stronger the updraft the more likely that precipitation particles will be suspended above the freezing level long enough for ¾-in hail formation. See the conceptual models of ordinary cell and multicell thunderstorms in Figs. 1, 2, and 4b.

The flare echo described by Wilson and Reum (1988) usually extends several miles from the back edge of the cell. If a flare echo is present, it can be easily found on the WSR-88D Doppler radar composite reflectivity product as shown in Color Plate A1.

The WSR-88D Doppler radar hail detection algorithm typically detects 53 to 79 percent of the severe hail storms (hail greater than or equal to ¾ in). Research done by Kessinger et al. (1995) shows that a low false alarm rate of 16 percent can be expected with the algorithm (software version prior to build 9).

Velocity signatures for detecting **hail** include storm top divergence and moderate to strong mesocyclones. Storm top divergence is simply the addition of the absolute value of the maximum inbound wind plus the maximum outbound wind at the top of the storm. The storm relative velocity product (SRM) is usually the favored product for storm top divergence. In Fig. 21, storm top divergence is plotted versus the probability of hail size. Storm top divergence is another indication of storm updraft strength.

Moderate to strong mesocyclone signatures (Fig. 22) can be used to issue severe thunderstorm warnings for hail (as well as damaging wind) if the middle level environmental winds or shear are not considered favorable for tornadoes, as discussed in Section 3.b and c.

Another depiction of criteria for storm top divergence (hail size) and mesocyclones is shown in Fig. 23 (OSF 1995).

The **vertically integrated liquid (VIL)** guideline for **large hail** is usually referred to as the "**VIL of the Day**," which is a locally determined VIL based on environmental conditions of the day. One graphical guideline to help determine the VIL of the Day is shown in Fig. 24 (Wilken 1994). This type of graph could be created for any area, based on local experience. Another reference for VIL of the Day is a study done by Paxton and Shepherd (1993). The latter study provides the following formula for VIL of the Day:

$$\textbf{VIL of the Day} = \mathbf{750 / [(T500+T400) / 2]} \qquad (3)$$

where T500 = absolute value of 500 mb temp(C), and T400 = absolute value of 400 mb temp(C) VILs of this value or higher would suggest hail ¾-in in diameter or larger.

The last guideline concerning VIL in this paper is the VIL density equation (Amburn and Wolf 1996):

$$\textbf{VIL density} = \mathbf{1000\ (VIL / Echo\ top)} \qquad (4)$$

where VIL density is in g/m^3; VIL is in kg/m^2; and Echo top is in meters (1 m = 3.28 ft). If the VIL density is 3.50 - 4.00 g/m^3 or higher, then hail will likely be ¾ in or larger in diameter.

Many sites have developed other local studies of using VIL for hail forecasting, but these will not be presented here.

(2) Strong straight line wind

The techniques for **strong straight line wind** are:

1. Bow echo/derecho signatures - Fig. 7 and Color Plate A2
2. Supercell signatures - Figs. 3, 4c, and Color Plate B1
3. Mini supercell signatures - Tables 1 and 2
4. Base velocity magnitude

The signatures for **strong straight line wind** (50 kt or higher) include bow echo/derecho type signatures depicted in Fig. 7 (Fujita 1978). As noted in Section 2. d, the bow echo configuration is formed by acceleration of flow from the rear to front at middle levels by horizontal buoyancy gradients (Fig. 8). At times bookend vortices, one cyclonic on the north end of the bow and one anticyclonic on the south end, will be visible on Doppler radar storm relative velocity (SRM) or base velocity data. In Color Plate A2, a 50-kt wind can be seen in the center of the bow echo about 40 mi east of, and moving away from, Shreveport. Bookend vortices are on both the north and south ends of the bow. The distance from the WSR-88D and the orientation of the bow echo storm to the radial of the Doppler radar beam must be considered in determining actual wind velocity. The warning meteorologist must also be aware of the possibility of isolated tornadoes occurring in the cyclonic bookend vortex.

Typical multicell and supercell signatures as depicted by the Lemon criteria (Fig. 20) can be used to warn for strong straight line wind. These would be used to indicate a potential for strong straight line wind in a storm when velocity data are not detecting strong winds at the time.

As observed by Burgess et al. (1995), with mini supercells it is not necessary to have large and tall supercells to produce damaging wind and tornadoes. However, there may not be a strong association between large hail and mini supercells as there is for traditional supercells. In mini supercells the maximum reflectivities are not much above 50 dBZ, tops are sometimes as low as 20,000 ft, and never higher than 30,000 ft. See the comparison of mini supercells to traditional supercells in Table 1 from Burgess et al. (1995).

	ROT VEL kt (m s^{-1})	DIA nm (km)	HGT ft (km)
MINI (L)	28.8 (15)	1.9 (3.5)	
TRAD (L)	44.7 (23)	2.9 (5.4)	
MINI	32.4 (17)	2.0 (3.7)	14,700 (4.5)
TRAD	48.6 (25)	3.3 (6.0)	29,600 (9.2)

(L) = Surface to 3280 ft (1 km) AGL

Table 1
Mature Stage Mini Supercell (Burgess et al. 1995)

The **WSR-88D velocity** signatures for **strong straight line wind** are seen directly from the Doppler radar base velocity data. Any low elevation angle base velocity region of 50 kt or higher is recommended as severe thunderstorm warning criteria. The estimated actual wind speed may be higher than the WSR-88D Doppler radar base velocity wind speed, if the actual wind direction is not along the radial. Surface winds may also be stronger (or weaker) than radar beam level winds, of course, and effects of range (beam width) should also be kept in mind.

Mesocyclone criteria are usually best depicted by the storm relative velocity product (SRM) on the WSR-88D, but not always. Base velocity occasionally may be superior. Both supercell and mini supercell signatures can be used to issue severe thunderstorm warnings for strong straight line wind. As a reminder, environmental factors that limit the formation of tornadoes should be considered when using mesocyclone data. If environmental factors are not favorable for tornadoes, then a severe thunderstorm warning should be considered instead of a tornado warning even for moderate to strong mesocyclones (see Section 3.b and c).

(3) Ordinary cell microburst

The techniques for **ordinary cell microburst** are:

1. Descending high reflectivity core aloft - Fig. 1
2. Middle level velocity convergence just above cloud base (along with high reflectivity core aloft) - Fig. 25 and Color Plate A3
3. Divergent winds near surface directly from base velocity or SRM velocity - Color Plate A3

The **ordinary cell microburst** is one of the most difficult meteorological phenomena to warn for. According to Roberts and Wilson (1989), there are four features that can be used as microburst predictors. These are (1) a **descending reflectivity core** aloft, (2) **increasing convergence within the low levels of the storm**, (3) a reflectivity notch, and (4) rotation. Rotation and reflectivity notches do not appear to be reliable microburst predictors unless the other two features of descending reflectivity core and increasing horizontal convergence are also present.

A schematic example of a descending high reflectivity core is shown in Fig. 1. When considering middle level convergence, it is important to note that a base velocity cross section must be oriented along a radial to show a valid velocity cross section signature for convergence or divergence (Fig. 25). SRM or base velocity at various elevation angles can also be used to detect middle level convergent winds. In Color Plate A3, Falk and Harrison (1996) show an excellent example of a wet-microburst detected by Doppler radar. In this example, the maximum convergent winds in the 6,000-10,000-ft elevation were detected 14 min prior to the maximum divergent winds at the surface. The convergent signature just above the base of the storm is a possible indicator that air will be forced down within the storm to the surface, at which a divergent signature of the microburst will appear. One mechanism to create a downward buoyancy is precipitation evaporation just under the cloud base.

As mentioned above, the divergent wind signature directly from base velocity (or SRM velocity) at the surface is also an indicator of a microburst, but this feature is only detected at close range as the microburst is occurring or just after it has occurred.

b. Tornado warnings

Tornadoes have been divided into two groups for this discussion. The first is **supercell tornadoes** and the second is **non-supercell tornadoes.** The Doppler velocity products for tornadoes will generally refer to the storm relative velocity product (SRM) instead of base velocity.

In the following discussion, references will be made to "strong mesocyclones." Each office will have to define what criteria will constitute a strong mesocyclone based on type of environment, distance from the radar, rotational velocity, diameter of the mesocyclone, time of year, type of storm, and local climatology of storms. For example, in Shreveport during the fall and winter months, a strong mesocyclone is considered to have (1) a velocity rotational signature in the low levels, (2) an SRM velocity of 50 kt or greater (or base velocity of 64 kt or greater), in either the inbound or outbound velocity, and (3) a rotational velocity of 36 kt or more. These may be changed as experience with the WSR-88D grows. (Criteria subject to change without notice!) **When the environment is favorable for supercells and tornadoes, strong consideration should be given to issuing a tornado warning instead of a severe thunderstorm warning for moderate to strong mesocyclones** (see Section 3.b and c).

(1) Supercell Tornadoes

The techniques for **supercell tornadoes** are:

(1) Supercell signatures:

a. Bounded weak echo region - Fig. 4
b. Hook echo - Color Plate B1
c. Strong mesocyclone plus favorable tornadic environment - Fig. 22 and Color Plate B1
d. Tornado vortex signature

(2) Mini supercell signatures - Tables 1 and 2

The first guidelines for **supercell tornadoes** are the Lemon criteria (Fig. 20). These include the presence of a bounded weak echo region or a hook echo in conjunction with peak middle level reflectivities (16,000 to 39,000 ft) of 46 dBZ or greater, middle level overhang, and highest echo top over the low level reflectivity gradient. These radar signatures are all indicative of a strong rotating updraft. These signatures will form on the inflow part of the storm, usually on the southeast to southwest side.

A strong mesocyclone (Fig. 22) may be visible in the SRM Doppler data near where a hook echo is on the low level reflectivity data. A good example of a hook echo is seen in Color Plate B1 near Lancaster, Texas, just south of Dallas. Mid-level overhang above the low-level reflectivity gradient can be seen by comparing B1a and B1b. A strong mesocyclone can be seen in the same area. Lancaster was hit by a devastating tornado as this supercell storm moved through the town. All of these supercell features correlate well with the conceptual model of a classic supercell seen in Figs. 3 and 4c.

The WSR-88D Doppler radar algorithm generated **tornado vortex signature (TVS)** is also a feature that can be used to issue **tornado** warnings, although this feature is only triggered by the strongest of mesocyclones, and perhaps, may only be seen after the tornado has touched down.

Mini supercells are also listed in the supercell section because they will also have many of the same reflectivity features of the supercell. One difference is that the mesocyclone will be weaker in the SRM velocity data as compared to a supercell. However, the mesocyclone will be smaller in diameter for the mini supercell, so a lower rotational velocity in the mesocyclone may be considered for a tornado warning with a mini supercell. In mini supercells with mesocyclone diameters of 2.0 nm or less, the rotational velocities in Table 2 could produce tornadoes (OSF 1995).

Range (mi)	Rotational velocity (kts)
5	44
25	42
45	38
65	36
85	34
105	31

Table 2
Mini supercell mesocyclone (diameter 2.0 nm)

(2) Non-Supercell Tornadoes

The techniques for **non-supercell tornadoes** are:

(1) A rapidly growing cell on a stationary or slow moving boundary, especially if there are kinks or bends on the boundary signifying cyclonic vorticity areas.

(2) A low level mesocyclone signature close to the radar (within 50 miles).

Another very difficult feature to warn for is the **non-supercell tornado**. Roberts and Wilson (1995) concluded that tornadoes associated with non-supercell thunderstorms occurred while the storms were in their rapid growth stage. The vertical vorticity for the tornadoes originated near the surface along boundary layer convergence lines. From Roberts and Wilson (1995), Color Plate B2 shows non-convective cyclonic vorticity areas (in purple) along a boundary. The vorticity intensified and stretched upward in concert with the rapidly developing storms. Areas where tornadoes occurred are shown by the letter T. These storms did not contain pre-existing middle level mesocyclones. The reader is referred back to the conceptual model of non-supercell tornadic storms in Fig. 9.

The guidelines for warning for **non-supercell tornadoes** include trying to detect a rapidly growing thunderstorm on a stationary or slow moving boundary (front or outflow boundary), in an area where there is cyclonic vorticity on the boundary. Within 50 miles of the radar, a low level mesocyclone may be detectable. The non-supercell tornado is probably not detectable beyond 50 mi from the radar site.

NOTE ON THUNDERSTORM RAINFALL:

This note is included as a reminder that a **flash flood warning** may be needed in areas that have had severe weather, and the threat of heavy rain to life and property should not be overlooked.

Thunderstorms—even those which do not meet severe criteria—may produce copious amounts of rainfall in a short time. Meteorologists should be aware that slow-moving supercells and/or training of echoes over the same area may be precursors to flash flooding or disastrous effects of excessive rainfall.

The WSR-88D Doppler radar products of 1-hr precipitation (OHP), 3-hr precipitation (THP), storm total precipitation (STP), and user selected precipitation (USP) can help determine where heavy amounts of rain may have occurred. Although radar estimated rainfall may have to be manually adjusted downward for hail or "bright band" freezing level overestimates, or upward for tropical rainfall, the location of the heaviest rain on these products is usually accurate. Many times the rainfall estimates on these products are also very accurate.

6. Conclusion

Techniques for issuing tornado and severe thunderstorm warnings have been published in many varying sources. This paper attempts to gather most of these published techniques in one source for easy reference to meteorologists tasked with issuing tornado and severe thunderstorm warnings with the WSR-88D Doppler radar. Many other local studies are available,and meteorologists should also consult these when making the warning decision. This paper is not intended to be the definitive study on the subject of issuing tornado and severe thunderstorm warnings, but should be a guide for quick and easy reference when needed.

Acknowledgements

This paper began as a research project for the fall 1995 Cooperative Program for Operational Meteorology (COMET)/Mesoscale Analysis and Prediction (COMAP) course for SOOs in Boulder. I would like to thank Dr. James Wilson and Dr. Rita Roberts of the University Corp. for Atmospheric Research for their guidance and assistance in the research for this paper. I appreciate the comments and suggestions of the reviewers including George Wilken (SOO, NWSFO Little Rock), Dr. Morris Weisman (NCAR), and Dr. James Wilson (UCAR). I would also like to recognize Lee Harrison (MIC, NWSFO Shreveport) for allowing me the time to complete the project.

SUMMARY OF TECHNIQUES

SEVERE THUNDERSTORM WARNING:

HAIL

1. Lemon criteria - Fig. 20.
2. Flare echo - Color Plate A.1
3. WSR-88D Doppler radar hail algorithm.
4. Storm top divergence - Figs. 21 and 23.
5. Moderate to strong mesocyclone with environmental factors that limit tornado development - Section 3 and Fig. 22.
6. VIL of the Day graph - Fig. 24.
7. VIL of the Day = 750 / [(T500+T400) / 2] where T500 and T400 are absolute values of temperature in C at 500 mb and 400 mb.
8. VIL density = 1000 (VIL / Echo top) where VIL density is in g/m^3; VIL is in kg/m^2; and Echo top is in m (1 m = 3.28 ft).

STRONG STRAIGHT LINE WIND

1. Bow echo/derecho signatures - Fig. 7 and Color Plate A2.
2. Supercell signatures - Figs. 3, 4c, 24, 31, and Color Plate B1.
3. Mini supercell signatures - Section 2.c (definition), Tables 1 and 2.
4. Base velocity magnitude (50 kt or higher with adjustments for actual wind direction off of the radial).

ORDINARY CELL MICROBURST

1. Descending high reflectivity core aloft - Fig. 1.
2. Middle level velocity convergence just above cloud base (along with high reflectivity core aloft) - Figs. 25 and Color Plate A3.
3. Divergent winds near surface on base velocity or SRM velocity - Color Plate A3.

TORNADO WARNING:

SUPERCELL TORNADOES

1. Bounded weak echo region - Fig. 4c.
2. Hook echo - Figs. 4c and Color Plate B1.
3. Strong mesocyclone plus favorable environment for tornadoes - Section 3 and Fig. 22 and Color Plate B1.
4. Tornado vortex signature.
5. Mini supercell mesocyclone - Section 5.b.1, Tables 1 and 2.

NON-SUPERCELL TORNADOES

1. A rapidly growing cell on a stationary boundary, especially if there are kinks or bends on the boundary signifying cyclonic vorticity areas - Color Plate B2
2. A strong low level mesocyclone signature close to the radar (within 50 miles) - Fig. 22 and Color Plate B2.

NOTE ON THUNDERSTORM RAINFALL:

Severe thunderstorms—and many which are not otherwise severe— can produce copious amounts of rainfall in a short amount of time. Meteorologists are reminded that a **flash flood warning** may be needed in areas that have had severe weather from slow moving thunderstorms, or in areas of train echo thunderstorms. Consult the WSR-88D Doppler radar products of one hour precipitation (OHP), three hour precipitation (THP), storm total precipitation (STP), and/or user selected precipitation (USP) for additional guidance on heavy rainfall areas.

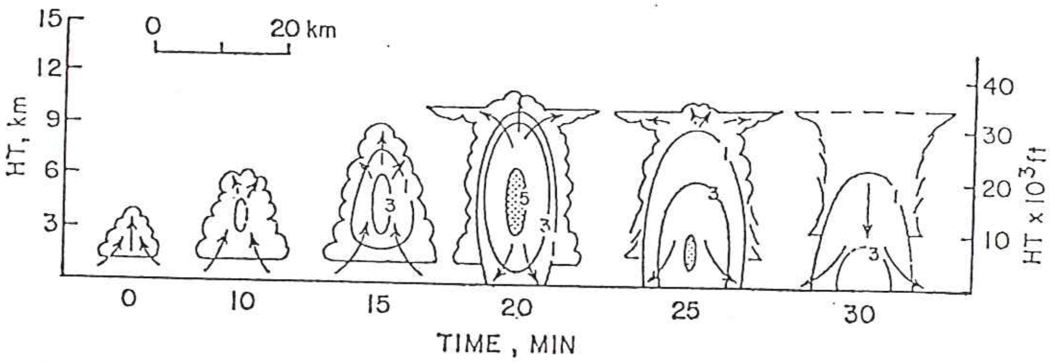

Figure 1 *Radar depiction of an ordinary thunderstorm, showing life cycle of radar cross section. Cloud features are schematic, while contours are at VIP levels.*

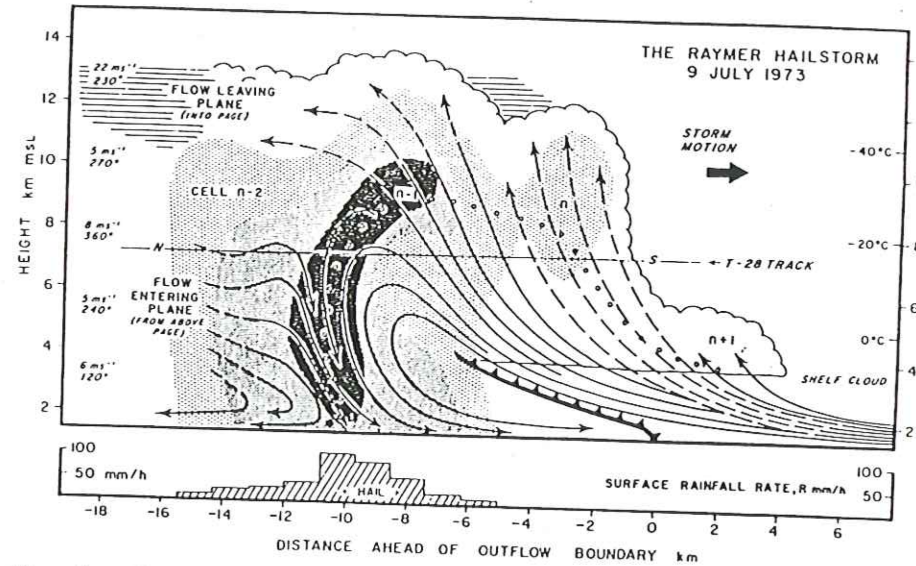

Figure 2 Vertical section of an ordinary multicell hailstorm, along the storm's direction of travel through a series of evolving cells (n−2, n−1, n, n+1). The solid lines are streamlines of flow relative to the moving system; on the left their broken ends represent flow into and out of the plane, and on the right they represent flow remaining within a plane a few kilometers closer to the reader. Light shading represents the extent of the cloud, and the three darker shades represent radar reflectivities of 35, 45, and 50 dBZ. (From Browning *et al.*, 1976.)

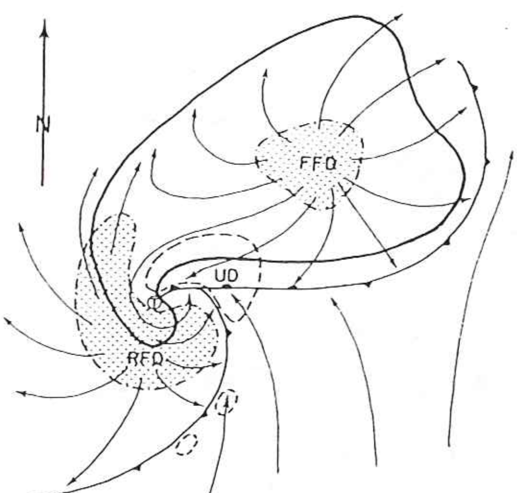

Figure 3 Plan view of a tornadic thunderstorm at the surface. Thick line encompasses radar echo. The thunderstorm "gust front" structure and "occluded" wave are depicted with a solid line and frontal symbols. Surface positions of the updraft (UD) are finely stippled; forward flank downdraft (FFD) and rear flank downdraft (RFD) are coarsely stippled; arrows are associated streamlines (relative to the ground). Encircled T is tornado location. (From Lemon and Doswell, 1979.)

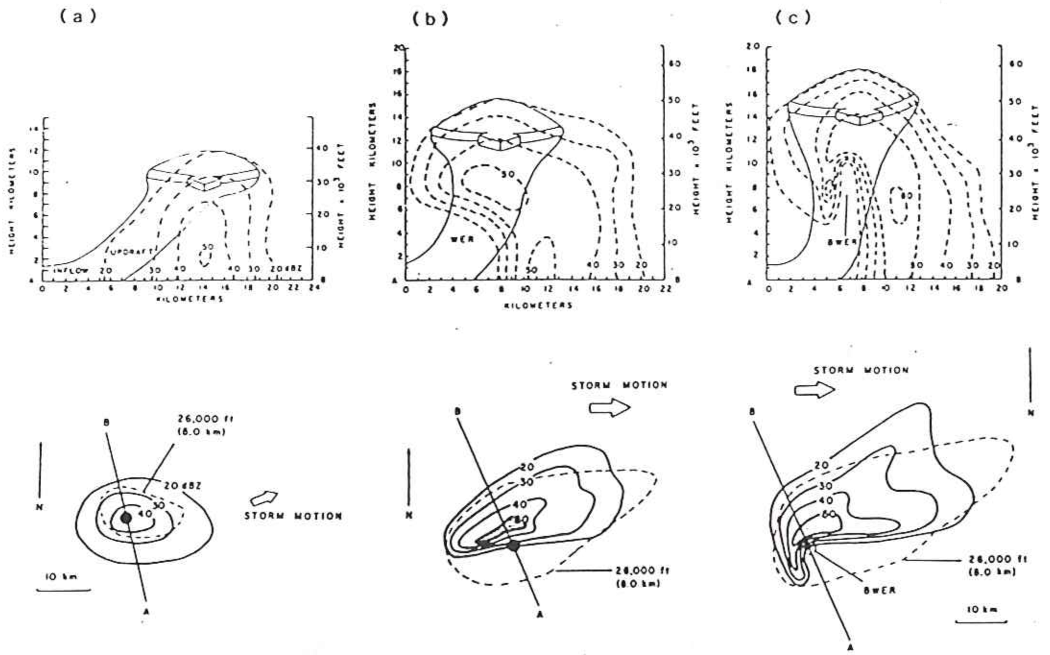

Figure 4 (Above) Vertical cross sections as might be observed on a radar scope during the (a) early, (b) middle, and (c) mature phases of a supercell storm. Low-level inflow, updraft, and outflow aloft (solid lines) are superimposed on the radar reflectivity (dashed lines). Reflectivities greater than 50 dBZ are stippled. The updraft becomes more intense as the storm evolves to its mature phase. WER implies a weak echo region and BWER implies a bounded weak echo region. (Below) Composite tilt sequences. Solid lines are the low-level reflectivity contours, dashed lines outline the echo >20 dBZ derived from the middle-level elevation scan, and the black dot is the location of the maximum top from the high-level scan. (Adapted from Lemon, 1980.)

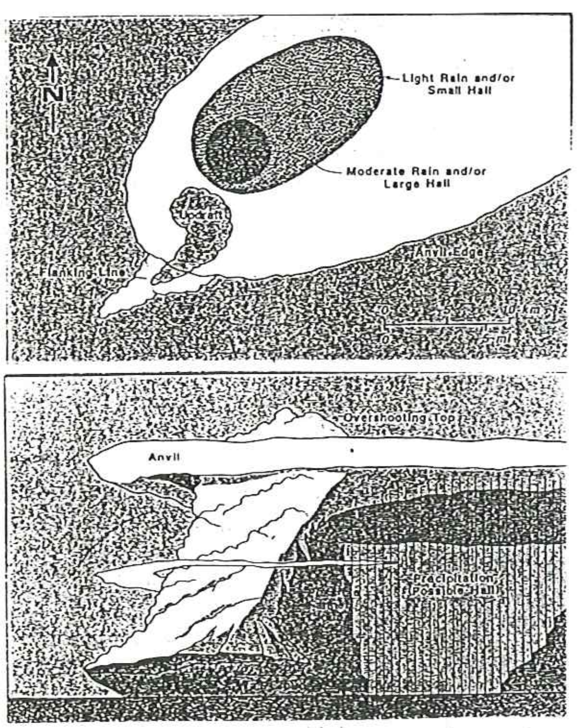

a

b

Figure 5 - Schematic for a LP supercell storm showing (a) a plan view looking from above showing precipitation (stippling), surface outflow boundaries, and cloud boundaries, and (b) an idealized view of the storm by a surface observer to the east. (Moller, et al., 1994)

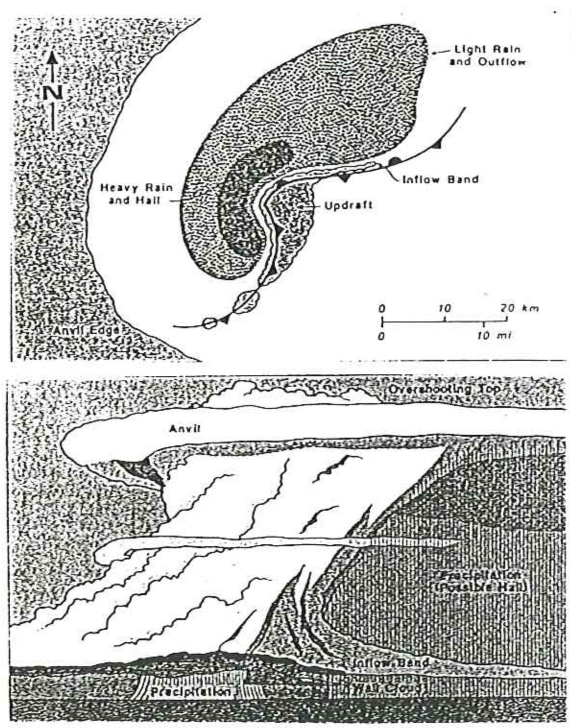

a

b

Figure 6 - Same as in Figure 5, except for a heavy precipitation storm. (Moller, et al., 1994)

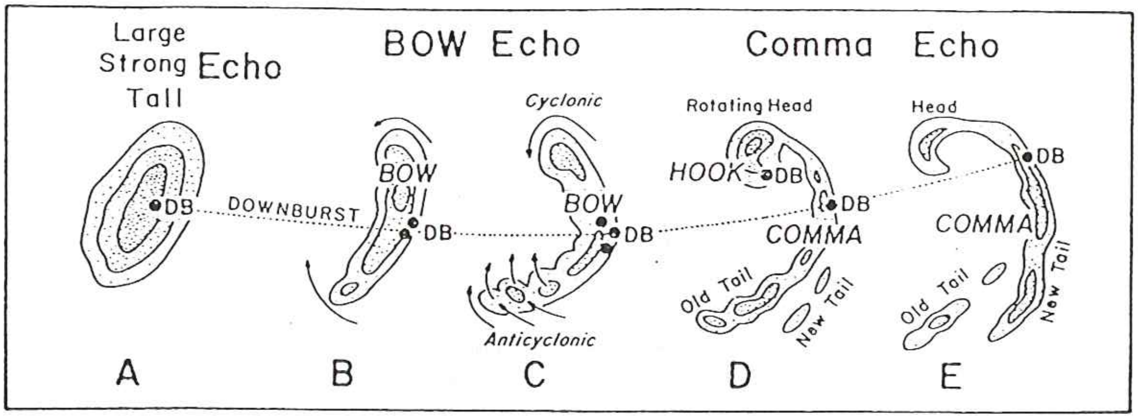

Figure 7 Typical evolution of a bow echo associated with strong straight line winds. DB (downburst) indicates area where strong winds may occur. Cyclonic and anticyclonic vortices (bookend vortices) are shown. Isolated tornadoes can occur in the cyclonic bookend vortex.

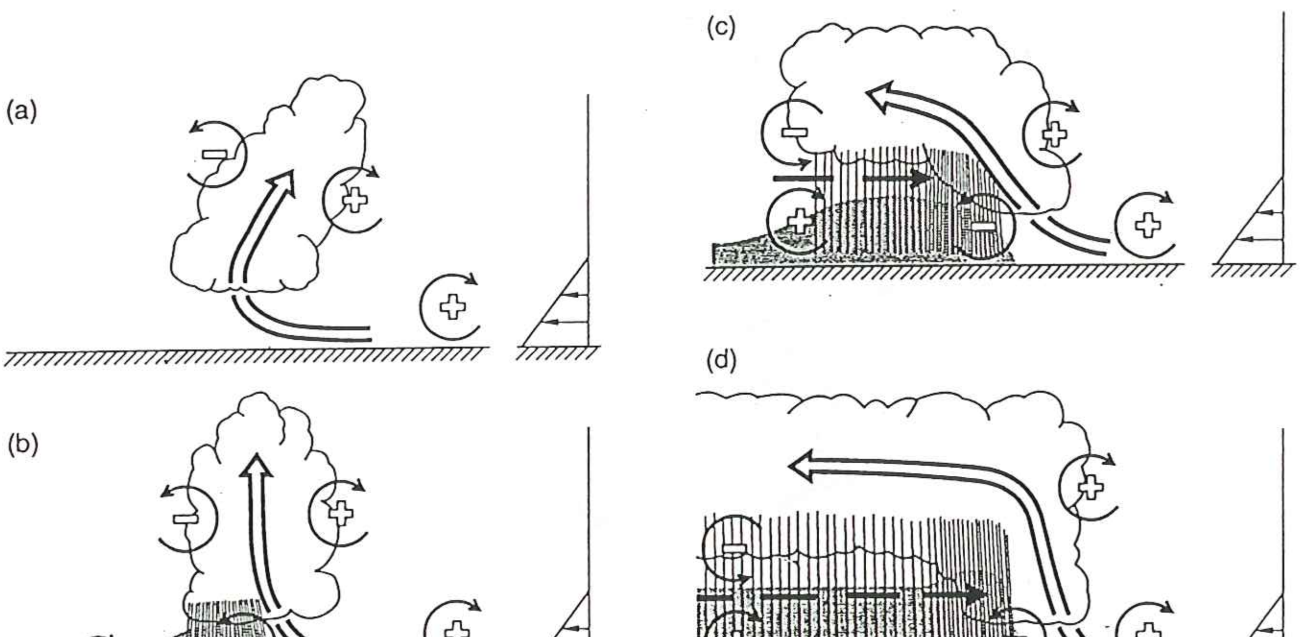

Figure 8 Four stages in the evolution of an idealized bow echo. (a) An initial updraft leans downshear in response to the ambient vertical wind shear, which is shown on the right. (b) The circulation generated by the storm-induced cold pool balances the ambient shear, and the system becomes upright. (c) The cold pool circulation overwhelms the ambient shear, and the system tilts upshear, producing a rear-inflow jet. (d) A new steady state is achieved whereby the circulation of the cold pool is balanced by both the ambient vertical wind shear and the elevated rear-inflow jet. The updraft current is denoted by the thick double-lined flow vector, with the rear-inflow current in (c) and (d) denoted by the thick dashed vector. The shading denotes the surface cold pool. The thin, circular arrows depict the most significant sources of horizontal vorticity, which are either associated with the ambient shear or are generated within the convective system, as described in the text. Regions of lighter or heavier rainfall are indicated by the more sparsely or densely packed vertical lines, respectively. The scalloped line denotes the outline of the cloud (adapted from Weisman 1992).

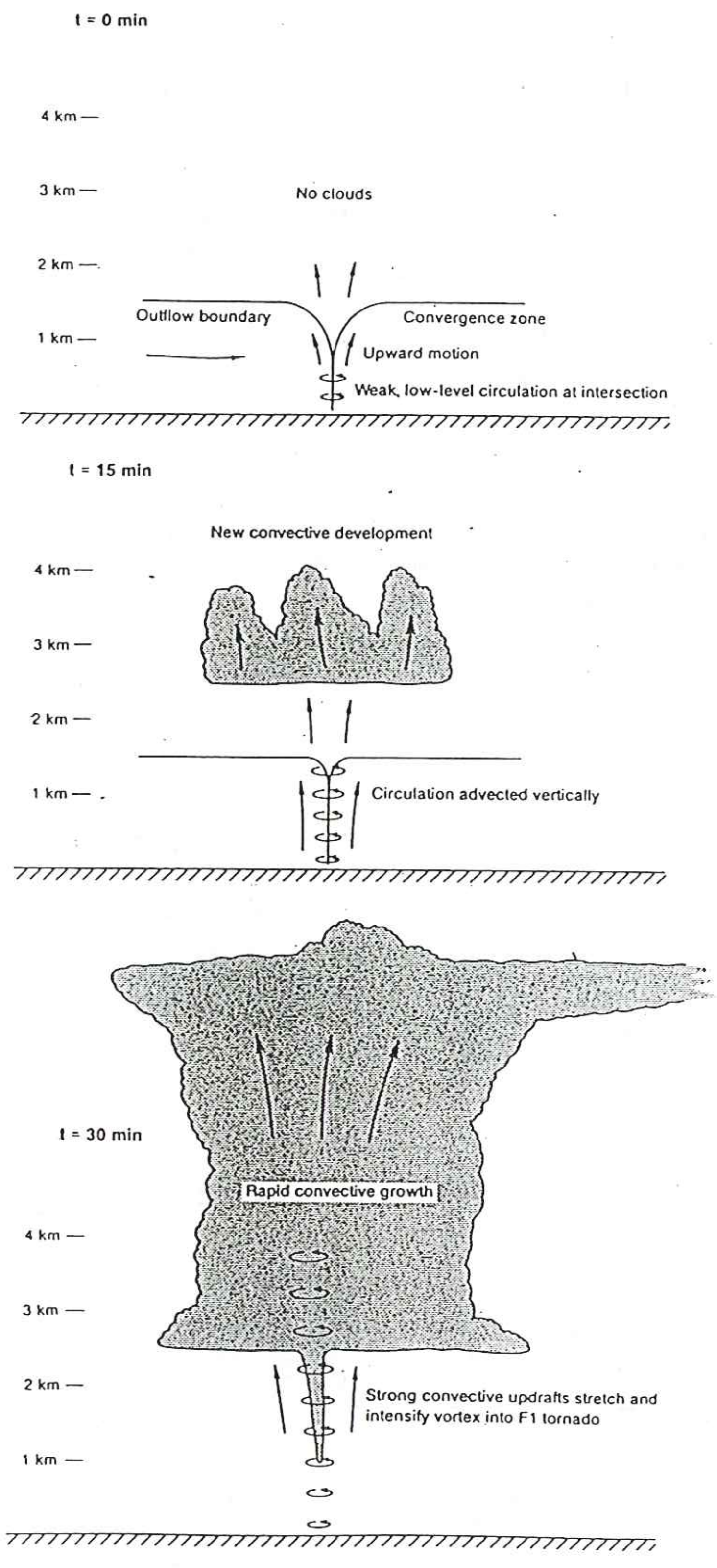

Figure 9 Basic scenario for most non-supercell tornadoes. The figure shows stretching of environmental vertical vorticity by the thunderstorm updraft in the growth stage.

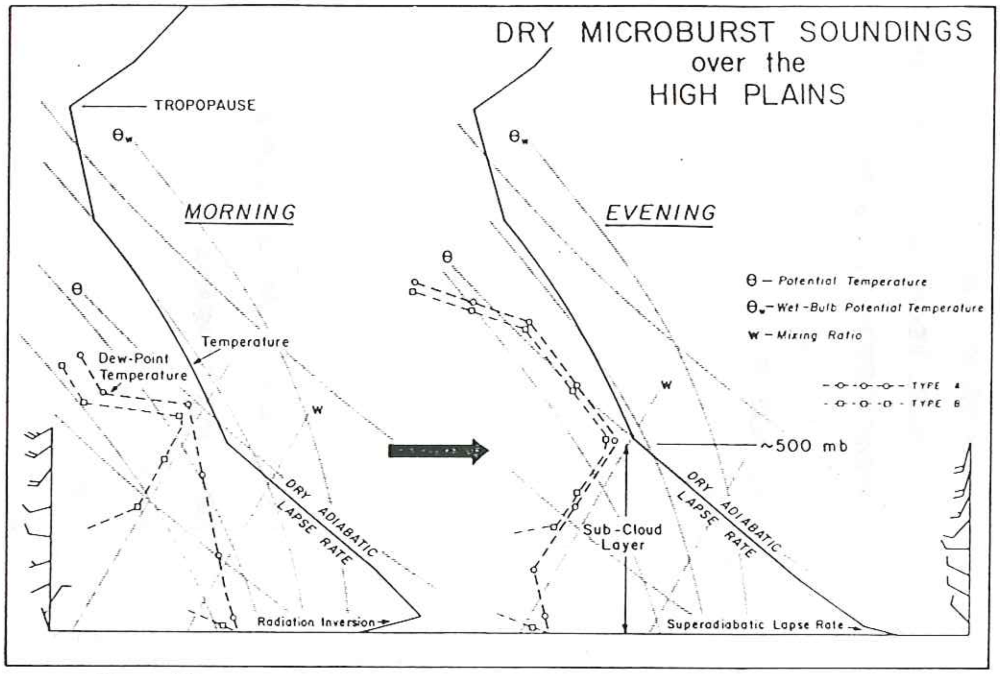

Figure 10a . Sounding model showing the environmental conditions favorable for dry-microburst activity over the High Plains (Fig. 8 from Wakimoto 1985).

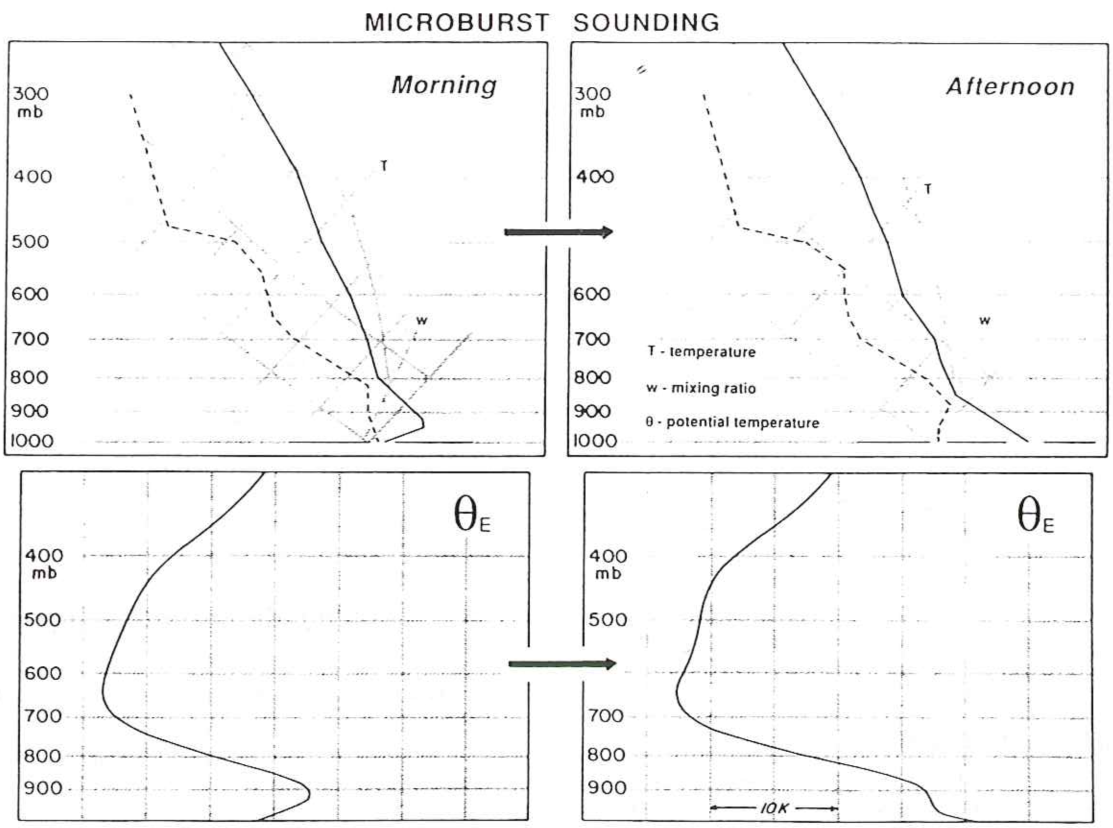

Figure 10b. Thermodynamic model summarizing the environment conducive for wet-microburst occurrence in a humid region.

(Atkins and Wakimoto, 1991)

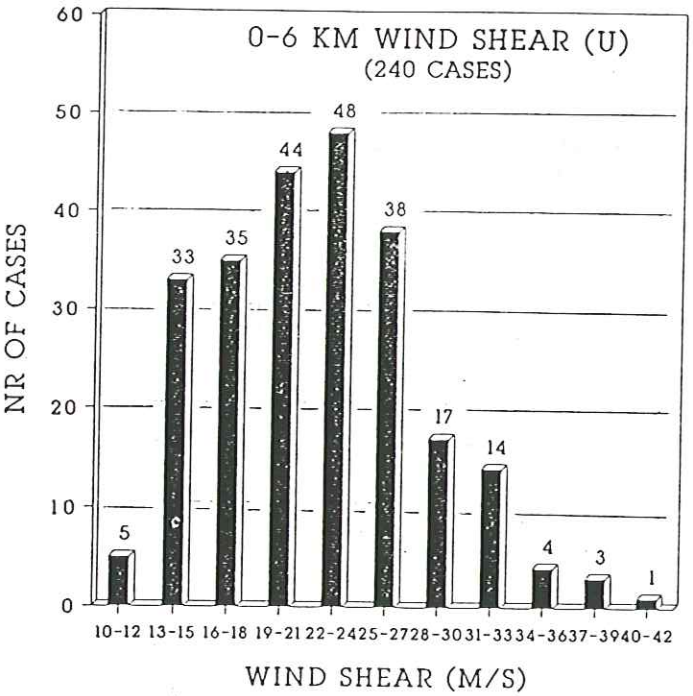

Figure 11 Distribution of cases from JDL data set, grouped according to *U* magnitude (Bulk Richardson Number shear) (in units of meters per second).

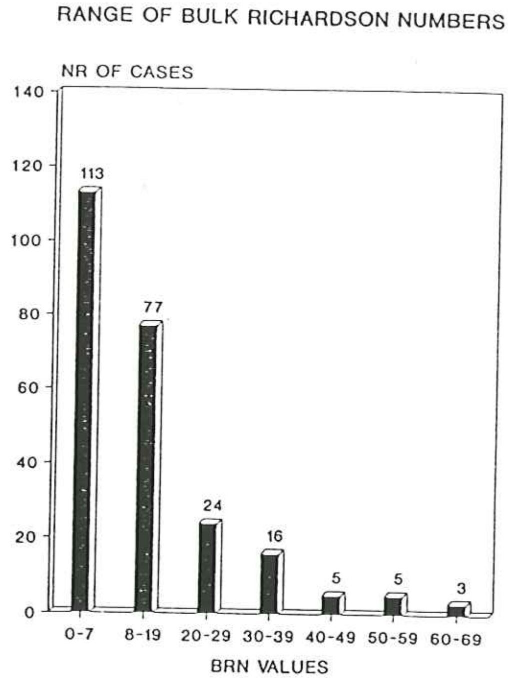

Figure 12 Distribution of Bulk Richardson numbers [*Weisman and Klemp*, 1982] for all 242 strong and violent tornado cases.

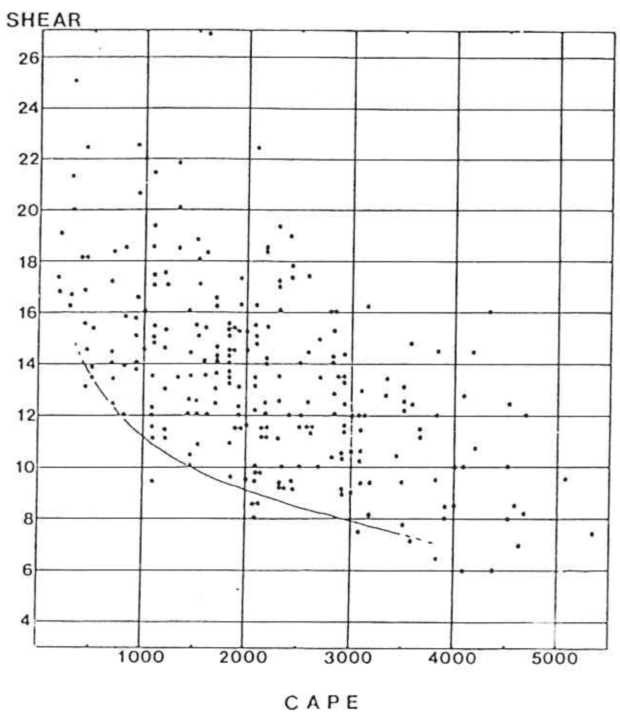

Figure 13. Scatter diagram showing the relationship between convectively available potential energy (CAPE) and 0-2 km AGL wind shear (X $10^{-3}s^{-1}$) for 242 tornado cases (Johns, et al., 1990).

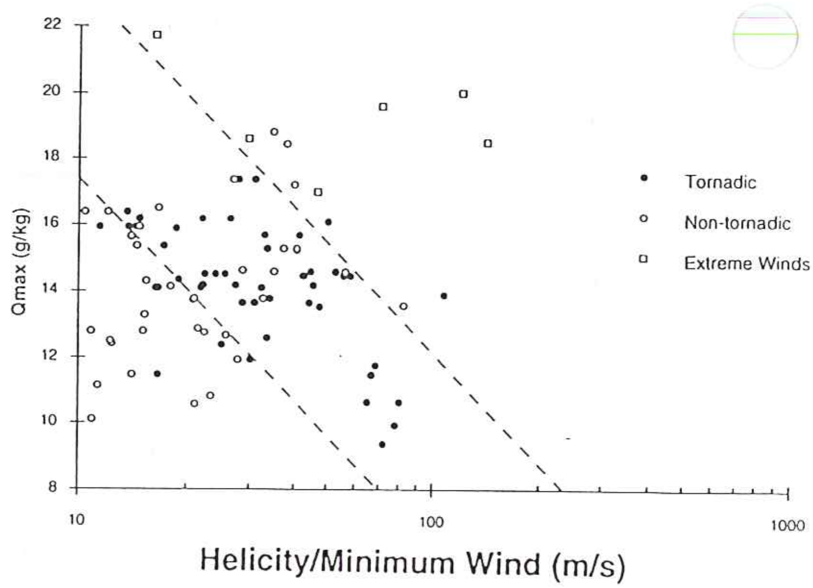

The H/v_{min} (m s^{-1}) and maximum water vapor content (q_{max}) in g kg^{-1} for proximity soundings. Note that horizontal axis is logarithmic. Dashed lines delineate three regions of environmental conditions

Figure 14
(Brooks and Doswell, 1994)

DERECHO CHECKLIST
(Pronounced day-ray-cho)

A. If <u>all</u> of the following five conditions are present in the area of interest, proceed to part B. Otherwise, derecho development is not likely.

	YES	NO
1. 500 mb flow direction 240° or greater?	___	___
2. Quasi-stationary boundary nearly parallel to 500 mb flow?	___	___
3. 850 mb warm advection within 200 nm?	___	___
4. 700 mb warm advection within 200 nm?	___	___
5. ELWS 25 kt or greater?	___	___

B. If <u>all</u> of the following three conditions are present in the area of interest, proceed to Part D. Otherwise, proceed to part C.

	YES	NO
1. Maximum 500 mb, 12 h height falls 60 m or greater? (50 m or greater at 0000 UTC?)	___	___
2. SELS lifted index -6 or lower?	___	___
3. ELRH < 80%?	___	___

C. If both of the following conditions are present in the area of interest, proceed to part D. Otherwise, derecho development not likely.

	YES	NO
1. SELS lifted index -8 or lower:	___	___
2. ELRH < 70% in initiation area (< 80% downstream?)	___	___

D. Do the parameter values satisfying the criteria for the SELS lifted index and the ELWS extend downwind along the quasi-stationary boundary for a distance of at least 250 nm from the convective system (or where the system is expected to develop)? If yes, go to E. If no, note that the potential for wind damage will probably be too localized to meet the areal criterion for a derecho. Nevertheless, forecasters in the affected area should be alert for the severe weather indicators listed in E.

E. <u>Be alert for derecho development</u>. If a convective system does develop, be particularly suspicious of any short squall line or squall line segment that moves at a speed of 35 kt or greater in the direction of the mean flow. Watch for satellite indications of damaging winds (McCarthy, 1985) and monitor radar closely for those signatures suggesting damaging winds or tornadoes (Lemon, 1980; Przybylinski and DeCaire, 1985).

CHECKLIST NOTES:

ELWS - Estimated Lower Midtroposophere Wind Speed; calculated by averaging the 500 and 700 mb wind speeds.

ELRH - Estimated Lower Midtroposphere Relative Humidity; the average relative humidity of the 500 and 700 mb levels. This can be found under AFOS header FRH69 for the LFM, and FRHT69 for the RAFS. In both products the R3 column can be used as an estimate.

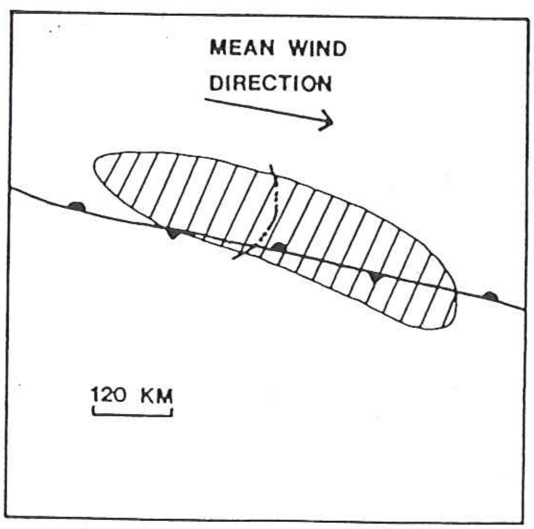

Schematic representation of features associated with a progressive derecho near midpoint of lifetime. Total area affected by derecho during lifetime indicated by hatching. Frontal and squall line symbols are convective.

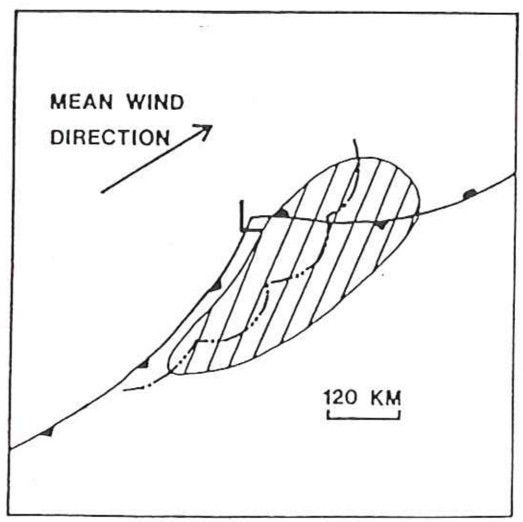

schematic representation of features associated with a serial derecho.

Figure 15
(Johns and Hirt, 1987)

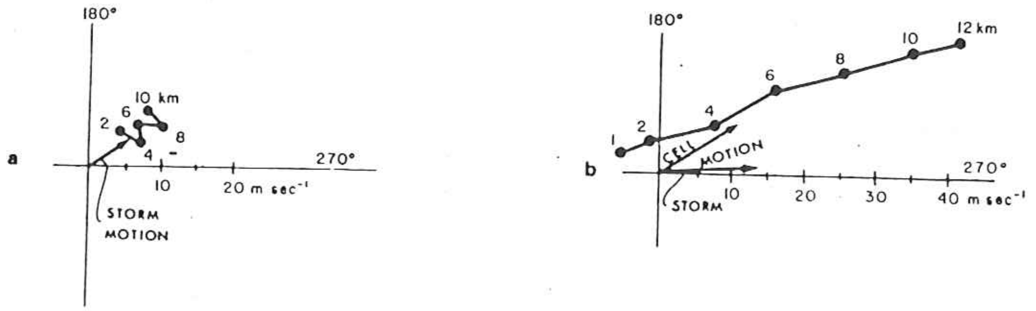

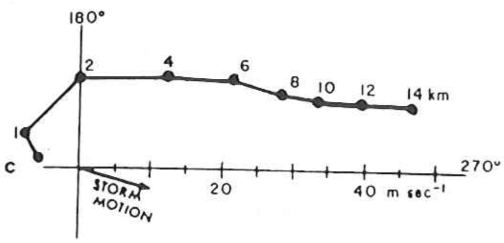

Figure 16 Typical wind hodographs for (a) single cell, (b) multicell, and (c) supercell storms observed during the Alberta Hail Studies project. (From Chisholm and Renick, 1972.)

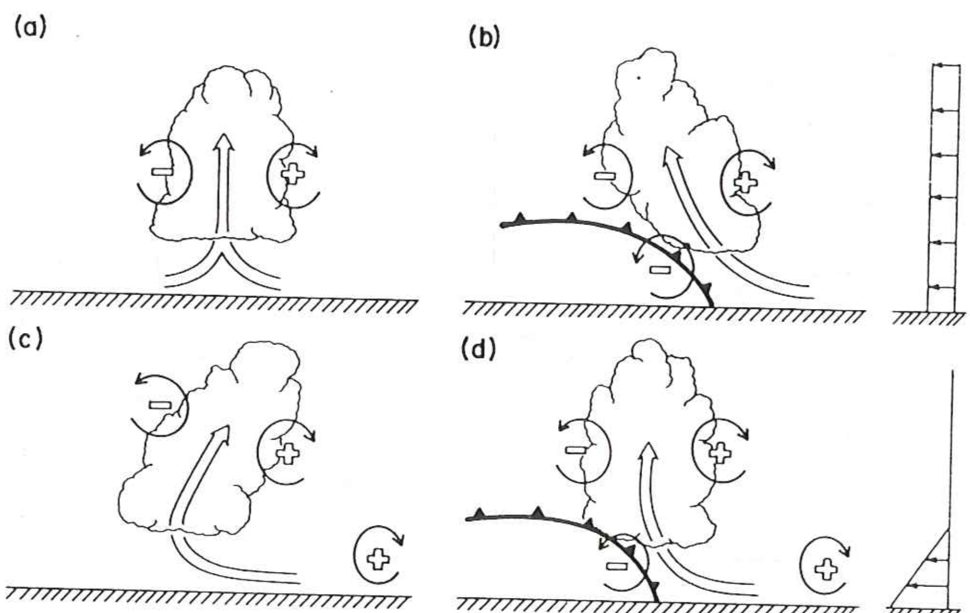

Figure 17 Schematic diagram showing how a buoyant updraft may be influenced by wind shear and/or a cold pool. (a) With no shear and no-cold pool, the axis of the updraft produced by the thermally created, symmetric vorticity distribution is vertical. (b) With a cold pool, the distribution is biased by the negative vorticity of the underlying cold pool and causes the updraft to lean upshear. (c) With shear, the distribution is biased toward positive vorticity and this causes the updraft to lean back over the cold pool. (d) With both a cold pool and shear, the two effects may negate each other, and allow an erect updraft.

(Rotunno, et al., 1988)

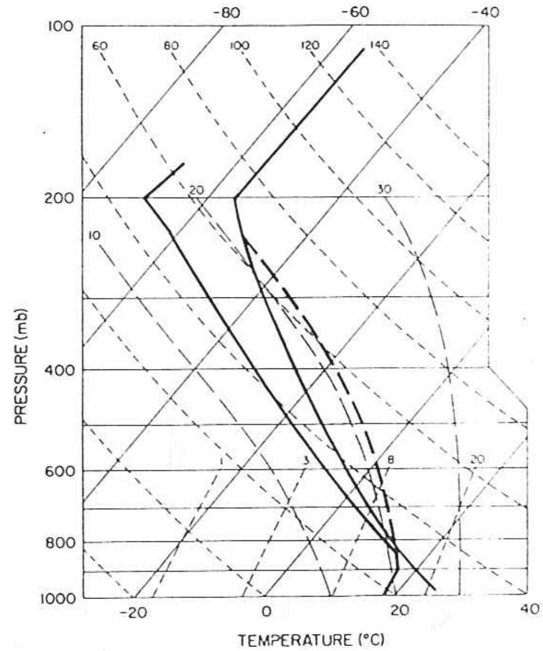

Figure 18 Skew-T diagram of temperature and moisture profile used in model experiments (heavy solid lines). Heavy dashed line represents a parcel ascent from the surface, based on a surface mixing ratio of 14 g kg^{-1} and a surface potential temperature of 300.7 K. The shaded region depicts the positive area defined by the parcel ascent. Tilted solid lines are isotherms; short-dashed lines are dry adiabats, and long-dashed lines are moist adiabats. (Adapted from Weisman and Klemp, 1982.)

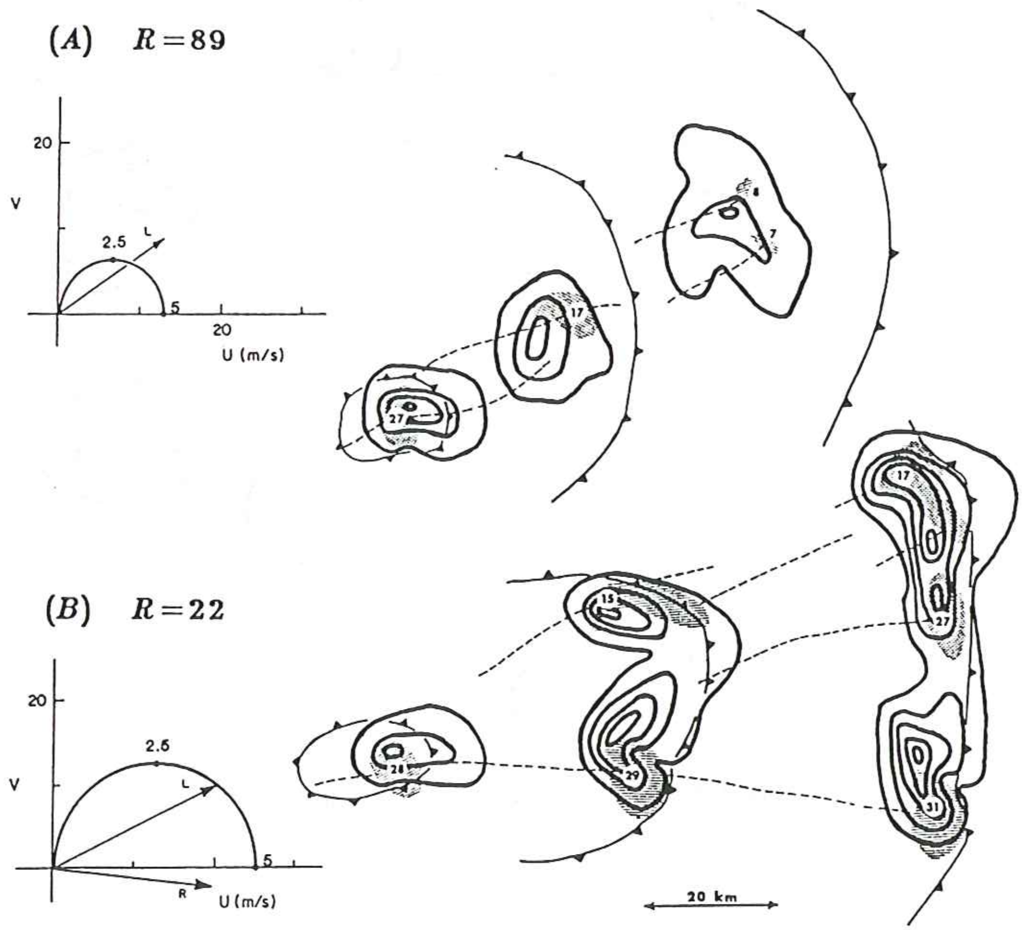

Figure 19 Hodograph and storm structures at 40, 80, and 120 min for cases A–F described in text. Storm positions are relative to the ground; dashed lines represent updraft cell path. Low-level (1.8 km) rainwater fields (similar to radar reflectivity) are contoured at 2 g kg^{-1} intervals. Regions in which the middle-level updraft (4.6 km) exceeds 5 m s^{-1} are shaded. Surface gust fronts are defined by the −1°C perturbation surface isotherm. Numbers at the updraft centers represent maximum vertical velocity (m s^{-1}) at the time. On hodographs, heights are labeled in km agl and arrows indicate the mean storm motion between 80 and 120 min. R = bulk Richardson number. Cases A and B, multi-cell and supercell storms.

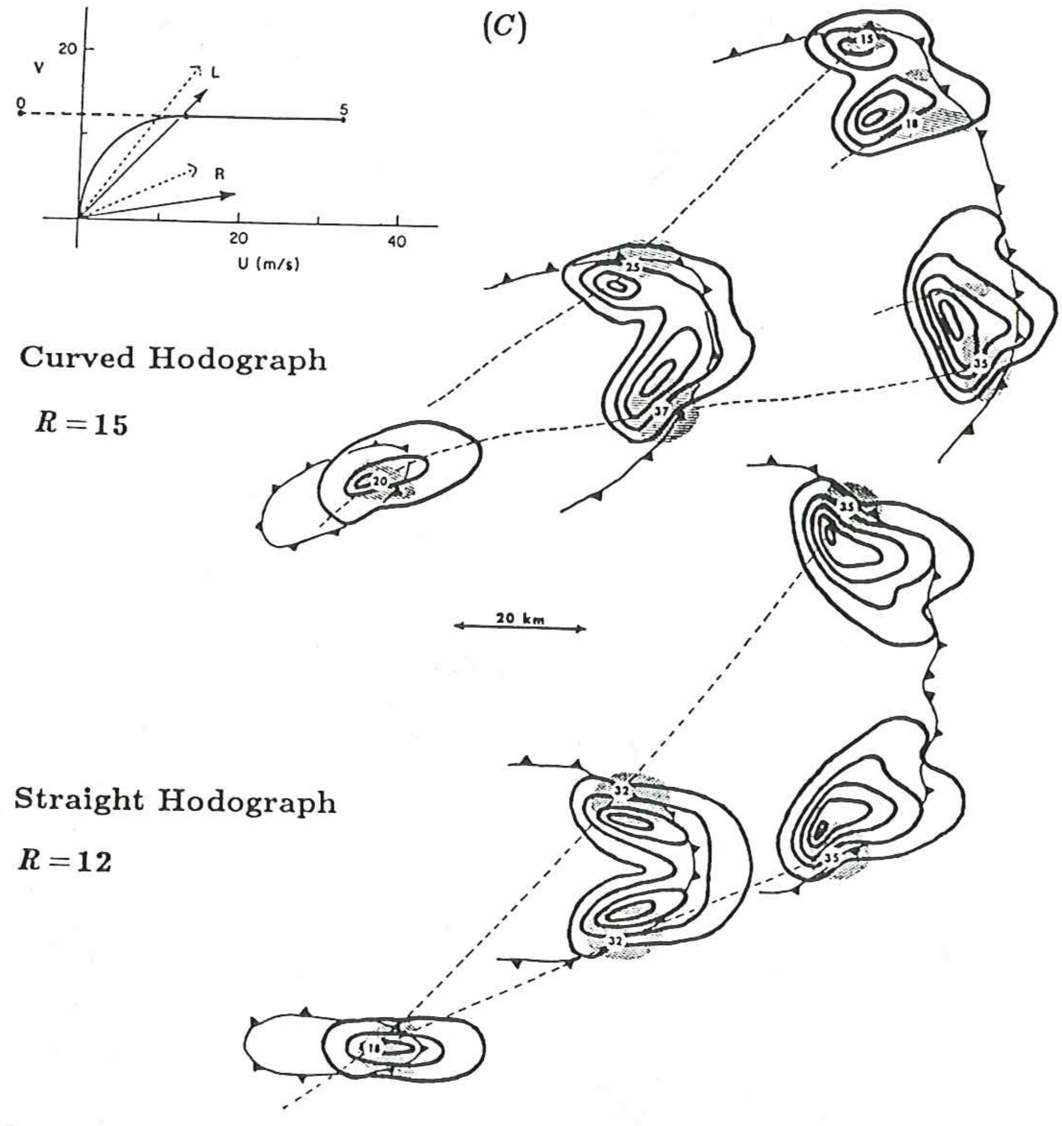

Figure 19 Continued. Case C, splitting supercell storms.

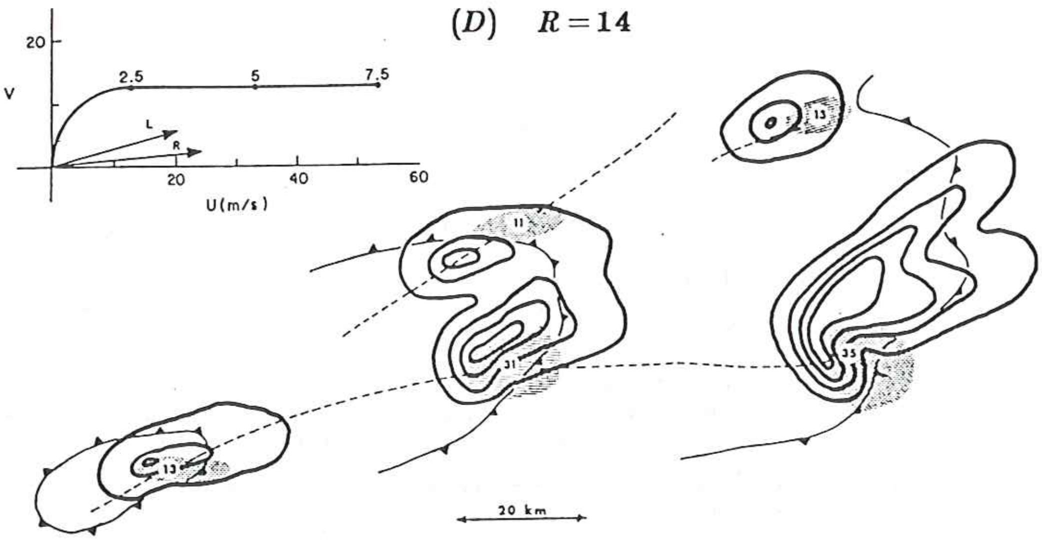

Figure 19 Continued. Case D, right-flank supercell.

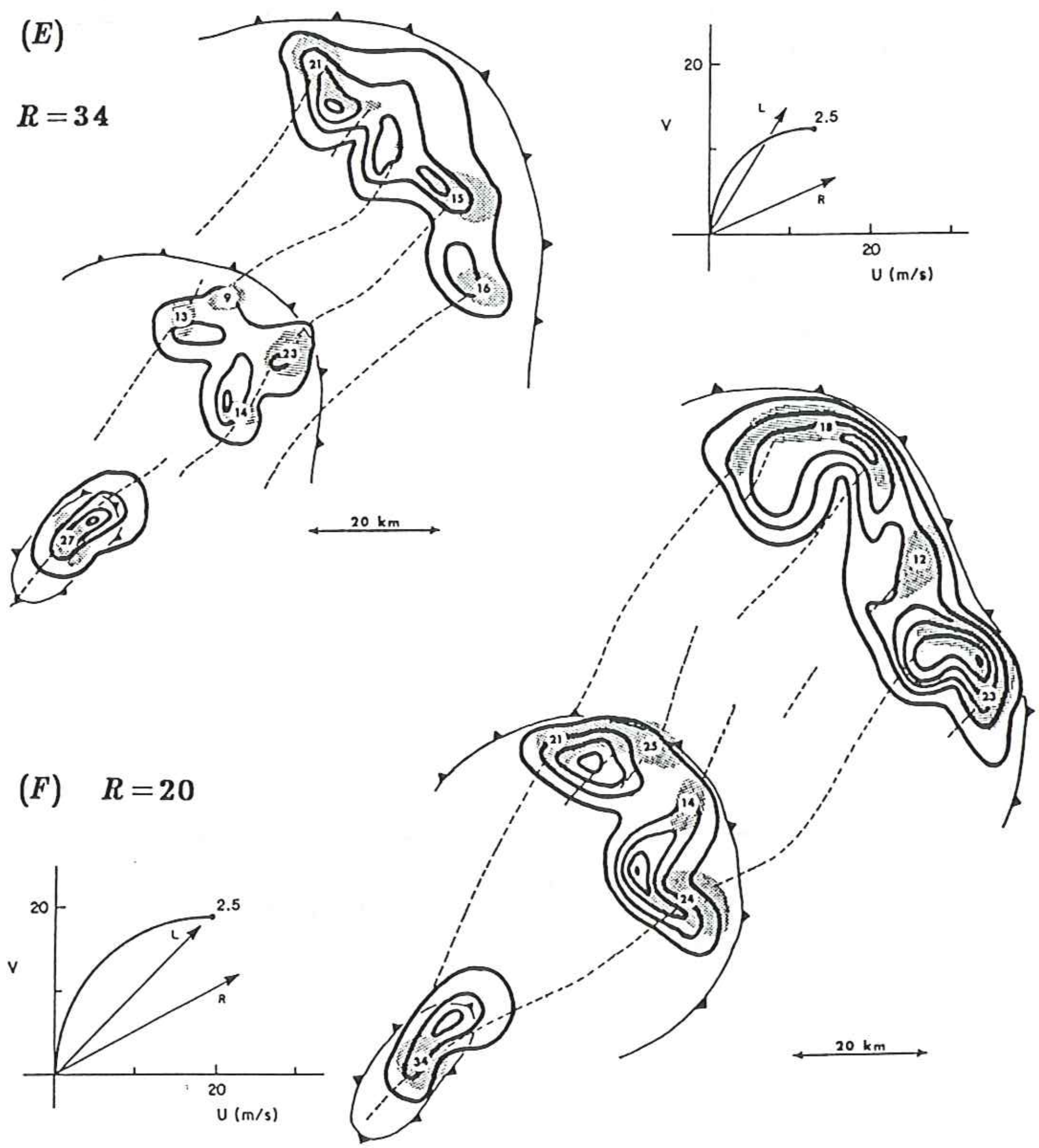

Figure 19 Continued. Cases E and F, multi-cellular squall lines.

In summary, the derived criteria for a severe thunderstorm warning are:

1. VIP 5 echo at 8 km (27,000 ft AGL) or higher.

In the absence of 1, all the following must be satisfied:

2. Peak mid-level (16,000 to 39,000 ft AGL) reflectivities must be ≥ VIP 4.

3. Mid-level echo overhang must extend at least 6 km beyond the outer edge of (or beyond the strongest reflectivity gradient of) the low-level (≤ 5,000 ft AGL) echo.

4. The highest echo top must be located on the storm flank possessing the overhang and be above the low-level reflectivity gradient between the echo core and echo edge or lie above the overhang itself.

Radar indication of a tornado requires the above 2, 3 and 4 criteria be satisfied and either or both:

1. A low-level pendant (oriented generally at right angles to storm motion) exists but may be embedded within lower reflectivities. (The pendent must lie beneath or bound the overhang echo on the west.)

2. A BWER (vault) is detected.

NOTE: VIP LEVELS OF EQUIVALENT REFLECTIVITY

Values in parentheses indicate threshold for next higher level (i.e., 45.7 dBZ would be VIP 3, 46.0 DBZ would be VIP 4.

VIP LEVEL	dBZ
1	0 - (30)
2	30 - (41)
3	41 - (46)
4	46 - (50)
5	50 - (57)
6	57 or more

Figure 20
Lemon Criteria for Warnings (Lemon, 1980)
and VIP levels equated to dBz.

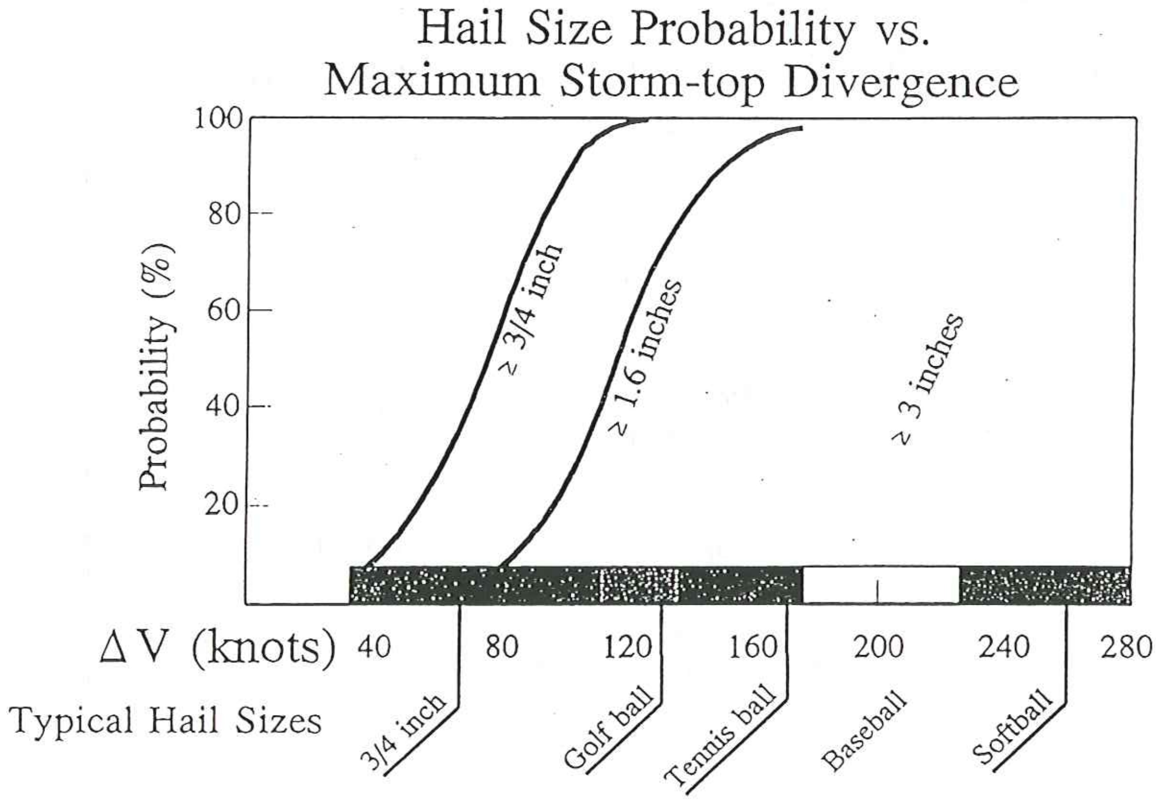

From Witt and Nelson (1991)
and NSSL (1985).

Figure 21

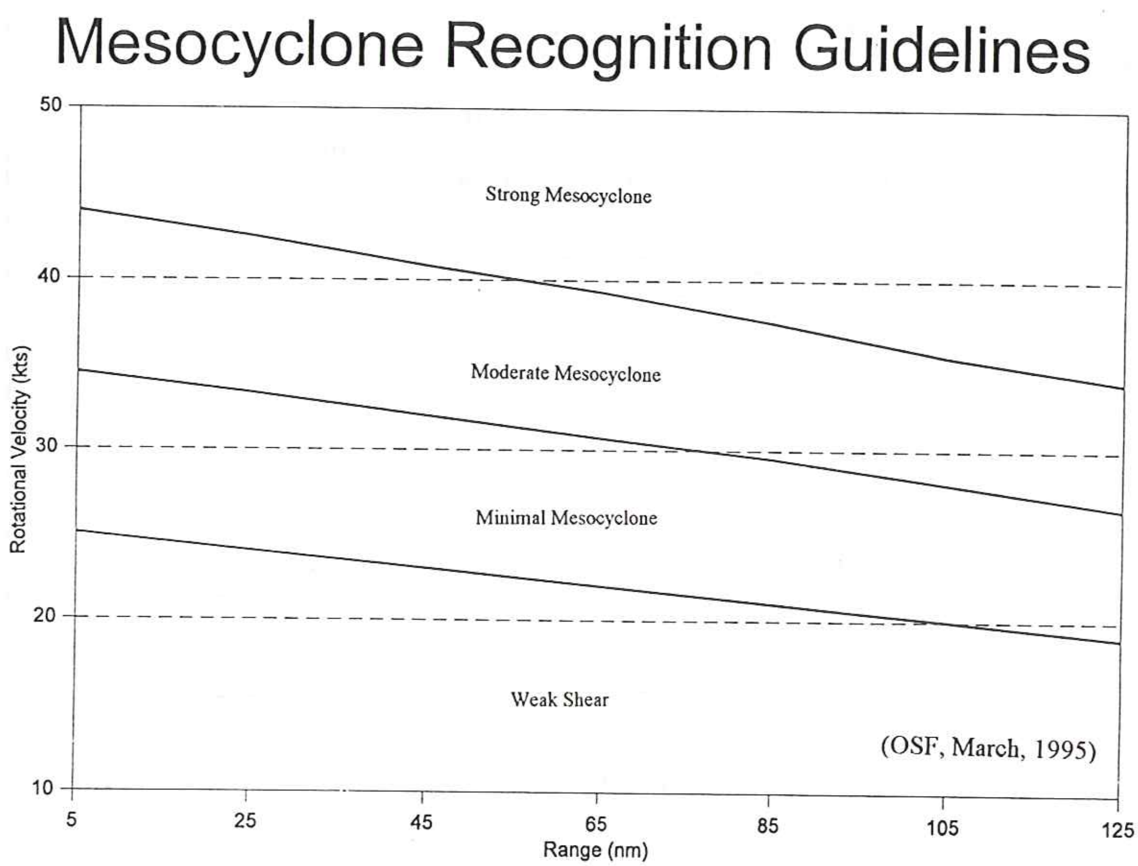

Figure 22 Mesocyclone recognition guidelines - for 3.5 nm diameter mesocyclones. If mesocyclone diameter is less than 3.5 mi, then lower rotational velocities may produce tornadoes. If mesocyclone diameter is larger than 3.5 mi, then stronger rotational velocities will be needed to produce tornadoes. In general, a tornado warning is recommended for a strong mesocyclone, and a severe thunderstorm warning is recommended for moderate or minimal mesocyclones. (OSF, March, 1995)

Storm Top Divergence and Maximum Hail Size

ΔV (knots)	Max Hail Size
≥ 75	Penny sized hail (3/4 in)
110 - 135	Golf ball (1.75 in)
135 - 175	Tennis Ball (2.25 in)
175 - 225	Baseball (2.60 in)
≥ 225	Softball/Grapefruit (4.00-5.00 in)

Criteria for determining possible hail size in storms based on the strength of the storm top divergence.

Mesocyclone Criteria for Warnings

SEVERE THUNDERSTORM WARNING

1. Rotational Velocity 25 to 44 kt if < 100 nm
   15 to 34 kt if ≥ 100 nm
2. Must have time continuity and vertical extent
3. Examine Base Reflectivity products, environmental conditions, and evaluate spotter reports.

TORNADO WARNING

1. Rotational Velocity ≥ 45 kt if < 100 nm
   ≥ 35 kt if ≥ 100 nm
2. Use other sources as described above

A guide for determining whether a severe thunderstorm or tornado warning should be issued based on rotational velocities and other factors.

(OSF, 1995)

Figure 23

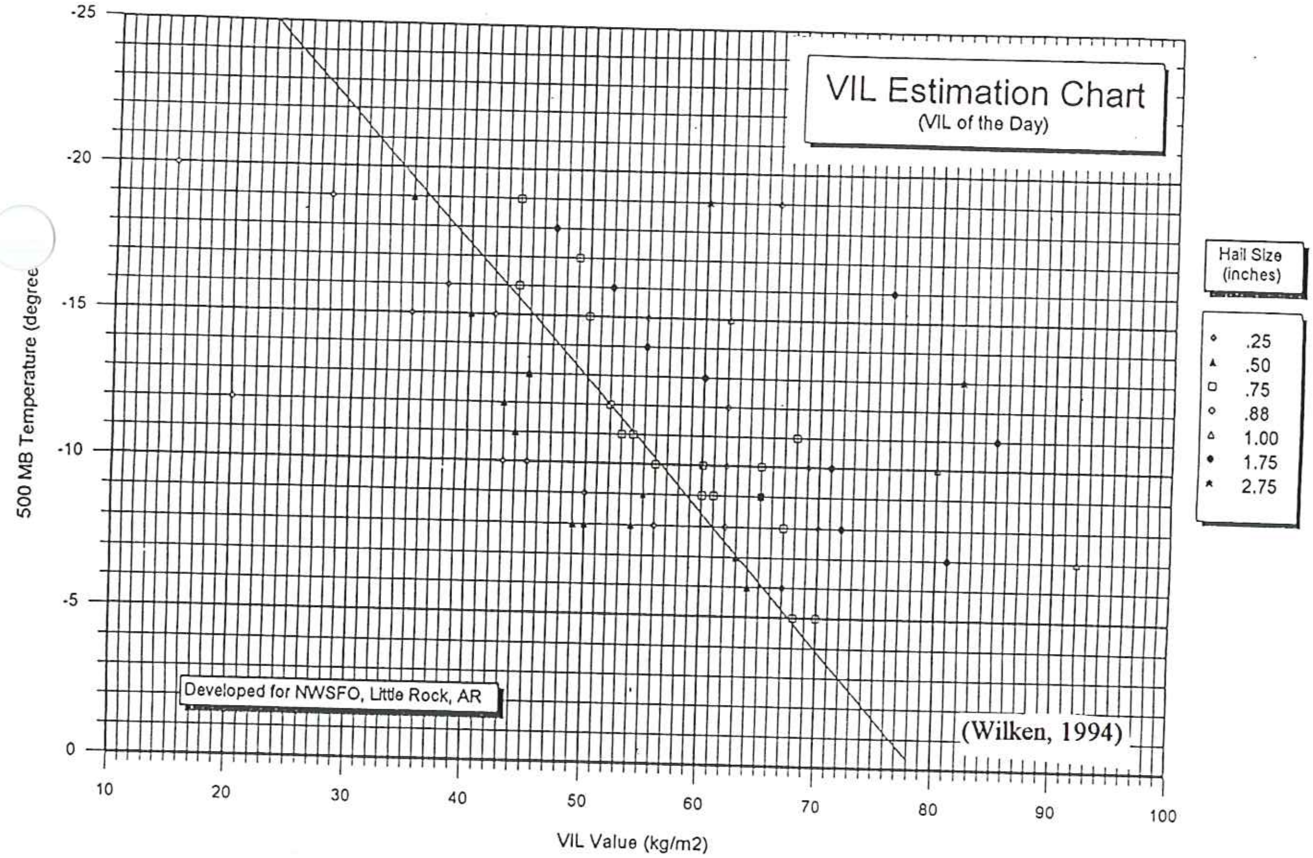

Figure 24

Figure 25

Proper base velocity cross section orientation for convergence/divergence.

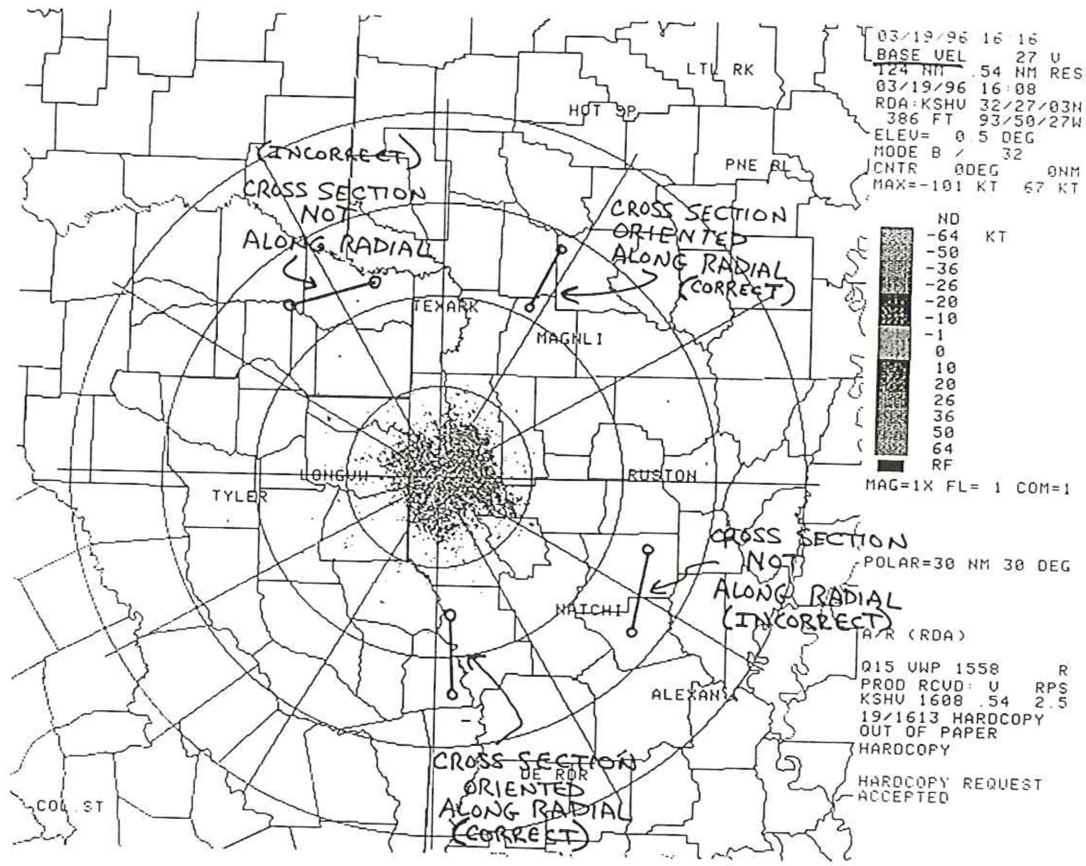

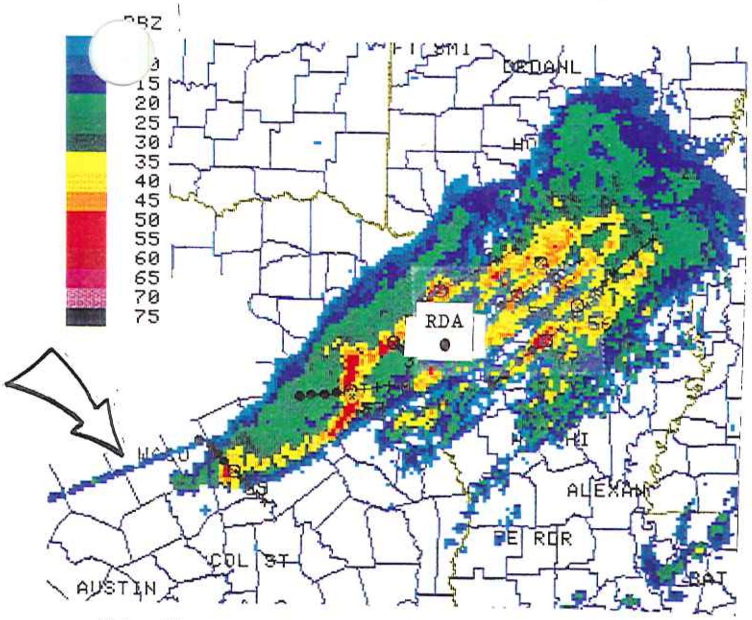

Color Plate A1. Flare echo shown on WSR-88D composite reflectivity product from Shreveport WSR-88D Doppler radar. RDA is just right of center, with intense hail-producing thunderstorm about 50 mi southwest of RDA.

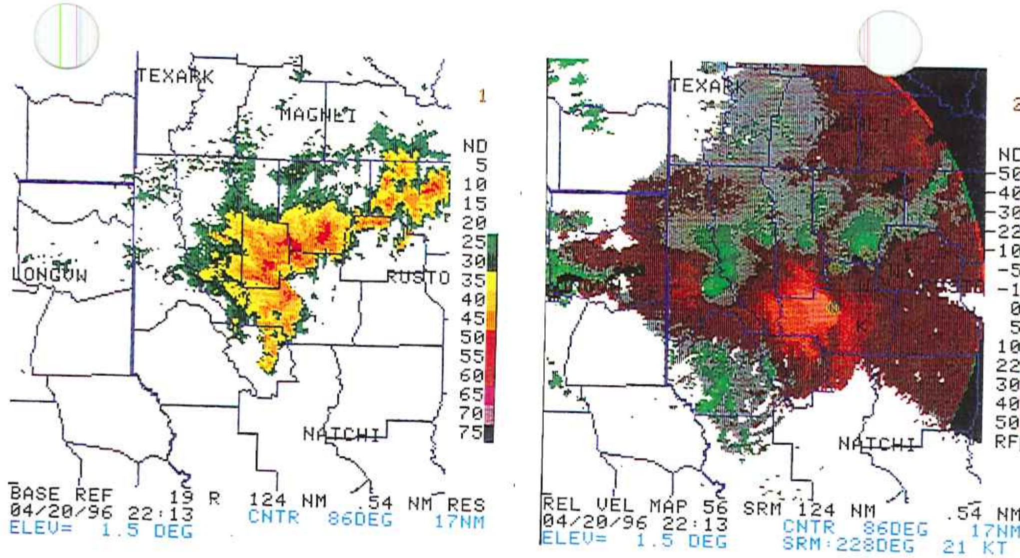

Color Plate A2. Bow echo on Shreveport WSR-88D Doppler radar. RDA is located just left of center. In (a) bow echo is about 50 mi east southeast of RDA. In (b) SRM WSR-88D product shows cyclonic bookend vortex on north side of bow and anticyclonic bookend vortex on south end. Strong straight line winds are indicated in the center of the bow echo.

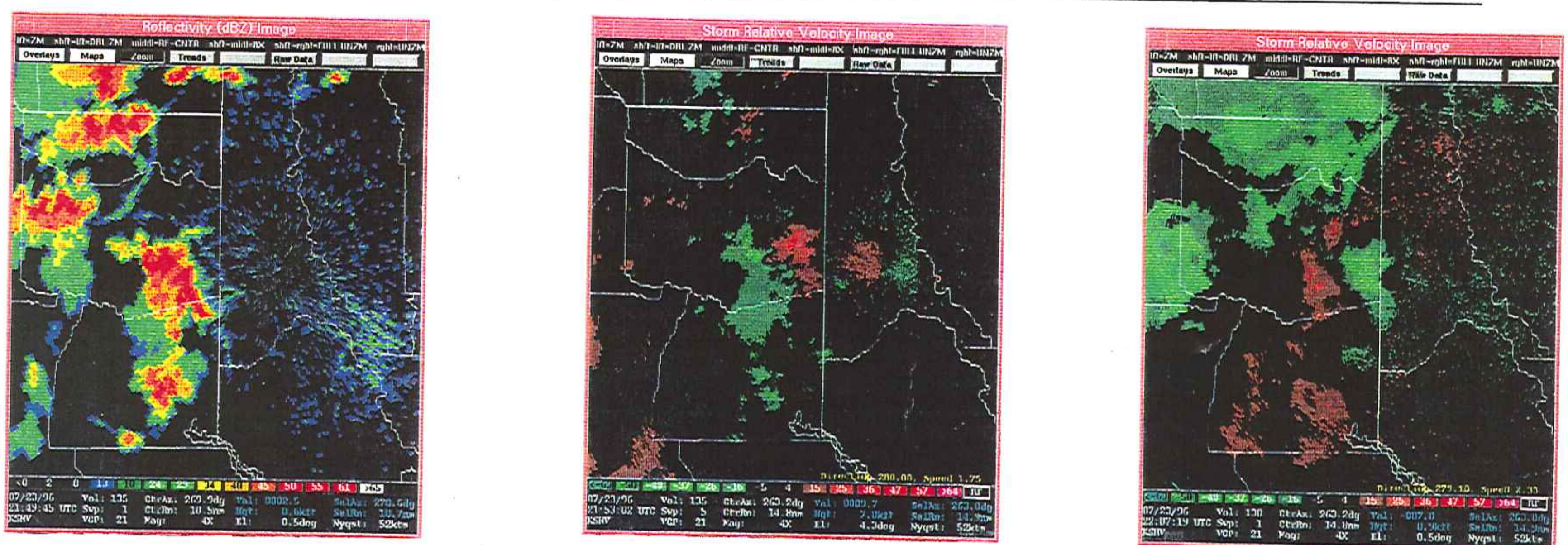

(a) Shreveport WSR-88D Doppler radar reflectivity at surface July 23, 1996, 2149 GMT. RDA is at right central part of figure.

(b) Shreveport WSR-88D Doppler radar SRM at 7000 ft, July 23, 1996, 2153 GMT. RDA is at right central part of figure. Note converging wind at Waskom, Texas, (15 mi west of RDA).

(c) Shreveport WSR-88D Doppler radar SRM at surface, July 23, 1996, 2207 GMT. Note diverging microburst winds at surface at Waskom, Texas, 14 min after maximum converging winds aloft (at 7000 ft) shown in Figure (b).

Color Plate A3

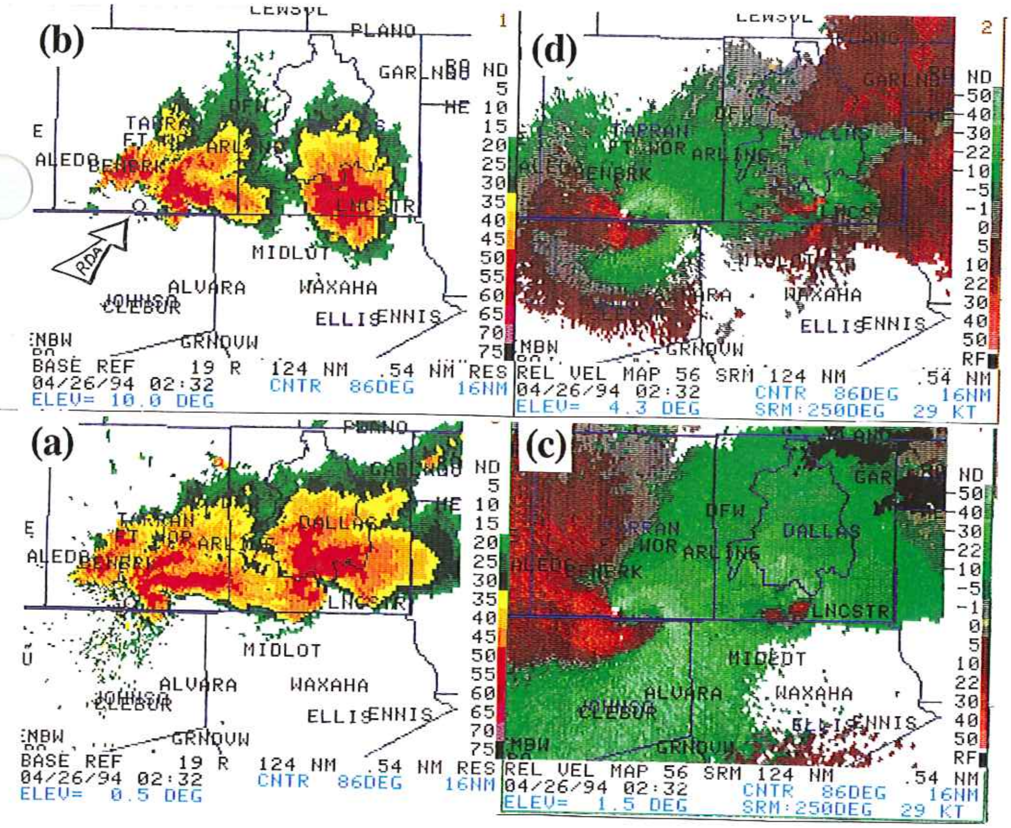

Color Plate B1

Tornadic supercell on Fort Worth WSR-88D Doppler radar. RDA is located just left of center. Figures (a) and (b) are reflectivity, and (c) and (d) are SRM. Note in (a) hook echo over Lancaster, Texas, just south of Dallas, (b) middle and upper level overhang over the low level gradient area, (c) mesocyclone over Lancaster, Texas, and (d) vertical extent of mesocyclone.

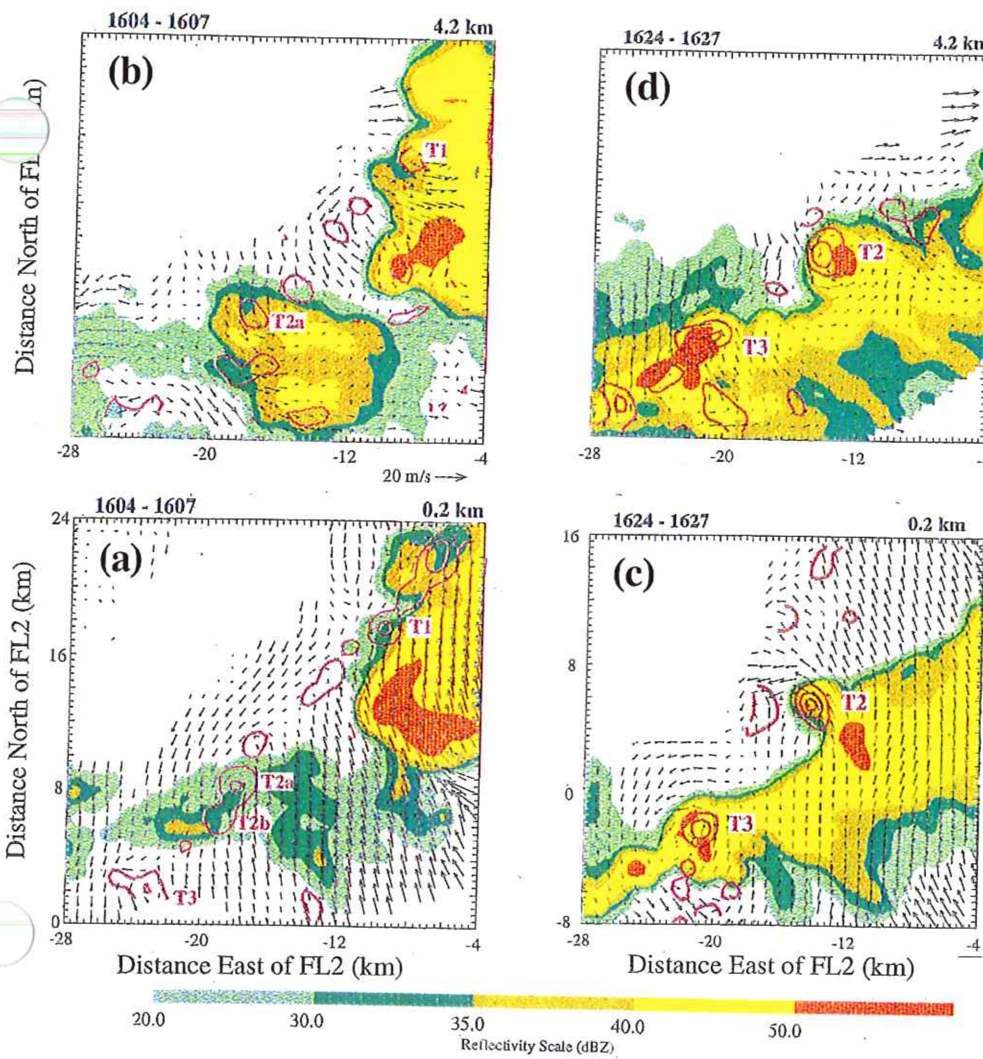

Color Plate B2

Reflectivity of non-supercell tornadic thunderstorms as shown by Lincoln Laboratory's FL2 Terminal Doppler radar, located just southeast of Denver Stapleton Airport. Tornado locations are shown by T1, T2a, T2b, and T3. Non-convective vertical cyclonic vorticity areas are in purple in increments of $10 \times 10^{-3} s^{-1}$ starting at $5 \times 10^{-3} s^{-1}$. Arrows indicate wind vectors, see scale under Figure (b).

REFERENCES

Amburn, S., and P. Wolf, 1996: VIL Density as a Hail Indicator. Preprints, *18th Conference on Severe Local Storms*, Amer. Meteor. Soc., 581-585.

Atkins, N. T., and R. M. Wakimoto, 1991: Wet microburst activity over the southeastern United States: Implications for forecasting. *Wea. Forecasting*, **6**, 470-482.

Atlas, D., 1990: Severe thunderstorm detection by radar. *Radar in Meteorology*, Amer. Meteor. Soc., 619-647.

Bluestein, H. B., and C. R. Parks, 1983: A synoptic and photographic climatology of low-precipitation severe thunderstorms in the Southern Plains. *Mon. Wea. Rev.*, **111**, 2034-2046.

Brady, R. H., and E. J. Szoke, 1989: A case study of nonmesocyclone tornado development in northeast Colorado: Similarities to waterspout formation. *Mon. Wea. Rev.*, **117**, 843-856.

Brooks, H. E., C. A. Doswell III, and R. B. Wilhelmson, 1994: The role of midtropospheric winds in the evolution and maintenance of low level mesocyclones. *Mon. Wea. Rev.*, **122**, 126-136.

Brooks, H. E., and C. A. Doswell III, 1994: On the environments of tornadic and nontornadic mesocyclones. *Wea. Forecasting*, **9**, 606-618.

Brown, J. M., K. R. Knupp, and F. Caracena, 1982: Destructive winds from shallow, high based cumulonimbi. Preprints, *12th Conference of Severe Local Storms*, San Antonio, TX, Amer. Meteor. Soc., 272-275.

Browning, K. A., J. C. Fankhauser, J. Chalon, P. H. Eccles, R. C. Strauch, F. H. Merrem, D. J. Jusil, E. L. May, and W. R. Sand, 1976: Structure of an evolving hailstorm. Part V: Synthesis and implications for hail growth and hail suppression. *Mon. Wea. Rev.*, **104**, 603-610.

Burgess, D. W., R. R. Lee, S. S. Parker, D. L. Floyd, and D. L. Andra, Jr., 1995: A study of mini supercells observed by WSR-88D radars. Preprints, *27th Conference on Radar Meteorology*, Vail, CO, Amer. Meteor. Soc., 4-6.

Chisholm, A. J., and J. H. Renick, 1972: The kinematics of multicell and supercell Alberta hailstorms. Alberta Hail Studies, *Research Council of Alberta Hail Studies*, Rep. 72-2, Edmonton, Canada, 24-31.

Colquhoun, J. R., and P. A. Riley, 1996: Relationships between tornado intensity and various wind and thermodynamic variables. *Wea. Forecasting*, **11**, 360-371.

Davies, J. M. and R. H. Johns, 1993: Some wind and instability parameters associated with strong and violent tornadoes 1. Wind shear and helicity. *The Tornado: Its Structure, Dynamics, Prediction, and Hazards*, American Geophysical Union, 573-582.

Doswell III, C. A., 1982: The operational meteorology of convective weather, Volume I: Operational Mesoanalysis. NOAA Technical Memorandum NWS NSSFC-5. NOAA National Severe Storms Forecast Center, Kansas City, MO.

Doswell III, C. A., 1985: The operational meteorology of convective weather, Volume II: Storm Scale Analysis. NOAA Technical Memorandum ERL ESG-15. NOAA National Severe Storms Lab, Norman, OK.

Doswell III, C. A., 1991: A review for forecasters on the application of hodographs to forecasting severe thunderstorms. *Natl. Wea. Dig.*, **16**, 2-16.

Doswell III, C. A., S. J. Weiss, and R. H. Johns, 1993: Tornado forecasting: A review. *The Tornado: Its Structure Dynamics, Prediction, and Hazards*, American Geophysical Union, 557-571.

Falk, K. W., and M. L. Harrison, 1996: Waskom, Texas, single cell microburst detected on National Weather Service Doppler radar - 23 July 1996. Technical Attachment SR/SSD 96-43, National Weather Service, Southern Region, Fort Worth, TX.

Fujita, T., 1978: Manual of downburst identification for Project NIMROD. SMRP Res. Paper No. 156, Univ. of Chicago, Chicago, IL.

Hart, J. A., and W. D. Korotky, 1991: The Sharp Workstation User's Manual. NOAA NWS National Weather Service Office, Charleston, WV.

Johns, R. H., and W. D. Hirt, 1987: Derechos: Widespread convectively induced windstorms. *Wea. Forecasting*, **2**, 32-49.

Johns, R. H., J. M. Davies, and P. W. Leftwich, 1990: An examination of the relationship of 0-2 km AGL "positive" wind shear to potential buoyant energy in strong and violent tornado situations. Preprints, *16th Conference on Severe Local Storms*, Kananaskis, Alberta, Canada, Amer. Meteor. Soc.

Johns, R. H., J. M. Davies, and P. W. Leftwich, 1993: Some wind and instability Parameters Associated with strong and violent tornadoes 2. Variations in the combinations of wind and instability parameters. *The Tornado: Its Structure, Dynamics, Prediction, and Hazards*, American Geophysical Union, 583-590.

Keighton, S., and J. Medlin, Operations Training Branch (OTB), Operational Support Facility (OSF), 1995: The WSR-88D Operator's Guide to Mesocyclone Recognition and Diagnosis.

Kessinger, C. J., E. A. Brandes, R. W. and Smith, 1995: A comparison of the NEXRAD and NSSL hail detection logarithms. Preprints, *27th Conference on Radar Meteorology*, Vail, CO, Amer. Meteor. Soc. 603-605.

Klemp, J. B., and M. L. Weisman, 1983: The dependence of convective precipitation patterns on vertical wind shear. Preprints, *21st Conference on Radar Meteorology*, Edmonton, Alberta, Canada, Amer. Meteor. Soc., 44-49.

Lemon, L. R., and C. A. Doswell III, 1979: Severe thunderstorm evolution and mesocyclone structure as related to tornadogenesis. *Mon. Wea. Rev.*, **107**, 1184-1197.

Lemon, L. R., 1980: Severe thunderstorm radar identification techniques and warning Criteria. NOAA Technical Memorandum NWS NSSFC-3. NOAA National Severe Storms Forecast Center, Kansas City, MO.

Moller, A. R., C. A. Doswell III, and R. Pryzybylinski, 1990: High precipitation supercells: A conceptual model and documentation. Preprints, *16th Conference on Severe Local Storms*, Kananaskis Park, Alberta, Canada. Amer. Meteor. Soc., 52-57.

Moller, A. R., C. A. Doswell III, M. P. Foster, and G. R. Woodall, 1994: The operational recognition of supercell thunderstorm environments and storm structures. *Wea. Forecasting*, **9**, 327-347.

OSF, 1995: WSR-88D Operations Training Student Guide. NEXRAD Operational Support Facility, Norman, OK.

Paxton, C. H. and J. M. Shephard, 1993: Radar diagnostic parameters as indicators of severe weather in Central Florida. NOAA Technical Memorandum NWS SR-149. NWS Southern Region, Fort Worth, TX.

Ray, P. S., 1986: *Mesoscale Meteorology and Forecasting*, Amer. Meteor. Soc., 793 pp.

Roberts, R. D., and J. W. Wilson, 1989: A proposed microburst nowcasting procedure using Single-Doppler radar. *J. Appl. Meteor.*, **28**, 285-303.

Roberts, R. D., and J. W. Wilson, 1995: The genesis of three nonsupercell tornadoes observed with Dual-Doppler radar. *Mon. Wea. Rev.*, **123**, 3408-3436.

Rotunno, R., J. B. Klemp, and M. L. Weisman, 1988: A theory for strong, long-lived squall lines. *J. Atmos. Sci.*, **45**, 463-485.

UCAR, COMET, 1996: Forecaster's Multimedia Library - A Convective Storm Matrix: Buoyancy/Shear Dependencies. University Corporation for Atmospheric Research (UCAR), Cooperative Program for Operational Meteorology, Education and Training (COMET), Boulder, CO.

Wakimoto, R. M., 1985: Forecasting microburst activity over the High Plains. *Mon. Wea. Rev.*, **113**, 1131-1143.

Wakimoto, R. M., and J. W. Wilson, 1989: Non-supercell Tornadoes. *Mon. Wea. Rev.*, **117**, 1113-1140.

Wakimoto, R. M., and B. E. Martner, 1992: Observations of a Colorado tornado, Part II: Combined photogram-meteric and Doppler radar analysis. *Mon. Wea. Rev.*, **120**, 522-543.

Weisman, M. L., and J. B. Klemp, 1982: The dependence of numerically simulated convective storms on vertical wind shear and buoyancy. *Mon. Wea. Rev.*, **110**, 504-520.

Weisman, M. L., and J. B. Klemp, 1984: The structure and classification of numerically simulated convective storms in directionally varying wind shears. *Mon. Wea. Rev.*, **112**, 2479-2498.

Weisman, M. L., 1992: The role of convectively generated rear-inflow jets in the evolution of long-lived meso-convective systems. *J. Atmos. Sci.*, **49**, 1827-1847.

Weisman, M. L., 1993: The genesis of severe, long-lived bow echoes. *J. Atmos. Sci.*, **50**, 645-670.

Weisman, M. L., 1996: On the use of vertical wind shear versus helicity in interpreting supercell dynamics. Preprints, *18th Conference of Severe Local Storms*, San Francisco, CA. Amer. Meteor. Soc.

Wilken, G. R., 1994: Estimating the "VIL of the day." Technical Attachment SR/SSD 94-50, National Weather Service, Fort Worth, TX.

Wilson, J. W., and D. Reum, 1988: The flare echo: Reflectivity and velocity signature. *J. Atmos. Oceanic Tech.*, **5**, 197-205.

Witt, A., and S. P. Nelson, 1991: The use of single-Doppler radar for estimating maximum hailstone size. *J. App. Meteor.*, **30**, 425-431.